Solvent Density Inhomogeneities in Supercritical Fluids

Susan C. Tucker

Department of Chemistry, University of California, Davis, California 95616

Received May 28, 1998 (Revised Manuscript Received November 13, 1998)

Contents

Susan C. Tucker is an Associate Professor of Chemistry at the University of California, Davis. She was born in Poughkeepsie, NY, in 1962. She received her B.A. in chemistry from Colgate University in 1984 (Phi Beta Kappa 1983) and her Ph.D. in physical chemistry from the University of Minnesota in 1989, where she worked with Donald G. Truhlar as an NSF Graduate Fellow. Her thesis work examined theoretical methods for evaluating Feshbach scattering resonances and the use of transition state theory in describing microsolvated ion-molecule reactions. As a postdoctoral associate with Bruce J. Berne at Columbia University from 1989 to 1991, she moved into the area of condensed-phase reaction dynamics, developing transition-state-theory-based descriptions of nonequilibrium solvent effects on solute reaction rates. Since her appointment to the faculty at Davis in 1991, she has continued to develop new theories for describing solvent effects on chemical reaction rates, with an emphasis on energy transfer controlled processes. Her research interests have also broadened to include the structure and dynamics of inhomogeneous supercritical fluids and supercritical fluid solutions, and much of her recent work has focused on the development of theoretical and simulation methodologies for characterizing such fluids and the dynamics of solutes within such fluids. She has been recognized with both an NSF Young Investigator Award and a Camille Dreyfus Teacher–Scholar Award, and she is presently (1999–2001) vice-chair of the Theoretical Subdivision of the American Chemical Society.

I. Introduction

A supercritical fluid (SCF) is here defined as any fluid which is at a temperature T greater than its critical temperature T_c, regardless of the pressure (or density). Historically,[1] the term SCF was reserved for cases in which the pressure P was also greater than the critical pressure, P_c, but this artificial distinction removes from consideration the very interesting behavior observed in lower pressure ($P < P_c$), high-temperature fluids. Supercritical fluid solvents make ideal candidates for use in the development of new chemical processes,[2−4] because thermodynamic condition can be used to control the solvating properties of these fluids. This thermodynamic control arises because the density of an SCF can be varied continuously from gaslike to liquidlike values by invoking modest changes in the pressure or temperature. Density-dependent solvent properties, such as the dielectric constant and viscosity, are thus also varied from gaslike to liquidlike values, causing corresponding changes in solute solvation. Of primary importance is the fact that states of intermediate density, where unexpected solvation and reactivity are observed,[2,4−8] may be accessed in SCFs. The novelty of solute behavior in this regime arises largely as a result of our general unfamiliarity with intermediate density solvents, our collective experience being based largely upon solute behavior in gases and liquids.

The greatest variation of solvent density is attained in the vicinity of the solvent's critical point, where the solvent compressibility is large, and small changes in pressure yield large changes in density.[9] Although this hypersensitivity can be problematic, making process control difficult, there is still much interest in understanding and predicting solute solvation and

10.1021/cr9700437 CCC: $35.00
Published on Web 01/15/1999

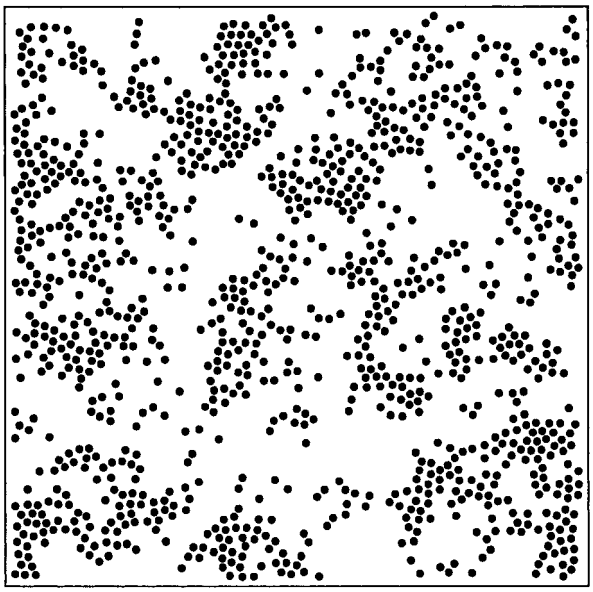

Figure 1. Configurational snapshot of a pure two-dimensional Lennard-Jones SCF at $T_r \approx 1.17$ and $\rho_r \approx 0.86$. (Details in ref 10).

reaction in the compressible regime around the solvent's critical point.

A large and growing body of evidence from the past decade suggests that when a solvent has a large macroscopic compressibility, κ, there are consequences at the microscopic level which may affect solute solvation, dynamics, and reactivity.[10] It has long been recognized that the magnitude of the compressibility is directly related to the range, ξ, over which microscopic fluctuations in fluid density are correlated, and that the divergence in the compressibility as $T \rightarrow T_c^+$ from above (along the critical scaling axis)[11] corresponds to a concurrent divergence of this correlation length ξ, i.e., the extension of these density fluctuations over macroscopic dimensions.[9,12] Hence, as one moves away from a solvent's critical point to higher temperatures and the compressibility decreases, the correlation length also decreases. Yet, in regions of large compressibility, i.e. $\kappa > \kappa^{IG}$, where κ^{IG} is the compressibility of an ideal gas under the same thermodynamic conditions, the correlation length may still extend over many molecular diameters, i.e. it may be of mesoscopic length. As a result, the instantaneous picture of an SCF in its compressible regime is that of an inhomogeneous medium with high and low-density regions extending over lengths of the order of the correlation length and smaller. Such inhomogeneities are evident in the molecular dynamics snapshot of a two-dimensional Lennard-Jones fluid[10] shown in Figure 1. One way to rationalize the existence of these regions of high and low density in an equilibrium, single-phase fluid is as follows: A large compressibility means that there is very little free energy cost to compression of the fluid. Microscopically, then, one expects that the free energy cost of density fluctuations is also low, and thus that the entropic cost of moving an isolated molecule onto a high-density region is nearly balanced by the energetic gain resulting from the increased number of favorable intermolecular interactions.

What happens when a solute is immersed in such an inhomogeneous medium? Work over the past decade has shown that for dilute SCF solutions, the *average* solvent density in the local region around a solute molecule will in general differ from the bulk density,[13] and that this deviation may be large, with typical increases/decreases on the order of 50−300%. More recently, a few studies have examined the fluctuation of the local solvent density around solutes, showing that around some solutes, the local solvent density fluctuations may be large, as they are in the pure SCF solvent. It is these solvent density inhomogeneities—both the average inhomogeneities, as well as their characteristics and fluctuations—which is the focus of the present review. As an aside, note that much work has been devoted to inhomogeneities which appear in solute−solute density distributions in highly compressible SCFs,[14−29] although this work will not be reviewed herein.

The body of the review begins with a brief discussion of the fundamental nature of solvent density inhomogeneities in infinitely dilute SCF solutions,[30,31] in order to enable the subsequent presentation of that evidence which supports the presence of such *local* solvent density inhomogeneities. These fundamentals have recently been explained in detail in ref 10, so only the basic elements will be presented herein. The comprehensive review of accumulated evidence for such inhomogeneities is organized according to the methodology used to detect such inhomogeneities. I begin by covering spectroscopic shift experiments, followed by equilibrium theoretical and computational treatments. I then examine the evidence for such inhomogeneities arising from dynamic measurements. Note that evidence of such inhomogeneities which arise from their effect on solute reaction rates, selectivities and equilibria will not be reviewed herein, as these topics are reviewed in another article in this volume, ref 32. Additionally, there are a handful of studies in which density inhomogeneities were not observed, and these studies are reviewed in a separate section. In the last section, I examine very recent work aimed at characterizing the nature of these density inhomogeneities. Note, however, that I do not cover studies examining specific molecular interaction effects, e.g. hydrogen bonding,[25,33−41] in compressible SCFs. Finally, this review provides comprehensive treatment of the aforementioned topics for the past decade, from 1989 to the present, and the reader is referred to earlier reviews[42−44] for coverage of the limited earlier literature.

II. Fundamentals

A. Local vs Long-Range Density Inhomogeneities

The first idea which must be addressed is the distinction between local and long-range average density inhomogeneities,[10,29,45−47] and we thus present a heuristical explanation of this distinction. A more formal discussion may be found in ref 10. While the present review will consider only local density inhomogeneities, the early literature does not make the distinction between local and long-range effects, and hence it can be both confusing and misleading if this

distinction is not clearly appreciated by the reader. This distinction also serves to further clarify the scope of this review.

In a highly compressible fluid, a solute may "induce" *average* solvent density inhomogeneities by two mechanisms. First, the solute may directly alter the number of solvent molecules within the range of the solute−solvent potential. That is, in a highly compressible solvent the cost of increasing the solvent density around the solute is minimal. Hence, the increased number of solvent−solute interactions created by moving solvent molecules into the range of the solute−solvent interaction potential more than offsets the cost of such a density fluctuation, and on average, the local solvent density will be enhanced relative to the bulk solvent density. Similarly, if the solvent−solute interaction is unfavorable, a solvent depletion within this interaction region will be energetically preferred. These average solvent density inhomogeneities, which are induced *directly* by solute−solvent interactions, have been called "direct density inhomogeneities".[10]

The second mechanism[48] by which solutes may "induce" *average* solvent density inhomogeneities is an indirect or nonlocal mechanism, resulting from the solvent−solvent density correlations present in the compressible fluid. Specifically, the direct solvent density enhancement (or depletion) created by the solvent−solute interactions can itself induce an *average* solvent density enhancement (or depletion) out to distances ξ, the correlation length of the solvent.[10,49] More explicitly, the direct solvent density enhancement (depletion) induces a tendency toward enhanced-density (depleted-density) fluctuations, because solvent density fluctuations out to distances ξ are, on average, correlated with the density fluctuation induced directly by the solute.[10] These indirectly induced solvent density inhomogeneities have been called "indirect density inhomogeneities".[10]

This mechanistic distinction is, however, heuristical, with no method for rigorously dividing observed enhancements into directly and indirectly induced components. (Note that the formal separation of solute-induced density enhancements in terms of direct and indirect correlation function integrals put forth by Chialvo and Cummings[47] cannot really be taken to provide such a separation of these mechanistic effects,[10,50] because the direct-correlation function integral cannot be physically interpreted as a density enhancement.) As a result, a more practical, although somewhat arbitrary, separation has become standard. Specifically, the average density enhancement observed around a solute in a compressible SCF is divided via an arbitrary spherical cutoff distance into a local and a long-range part. Within the solvent's compressible regime, the local and long-range components of the density inhomogeneitiy can be *approximately* equated with the direct and indirect components, as follows. If the cutoff is taken to be on the order of the range of the solute−solvent intermolecular potential, the local density component will incorporate all of the direct effects (plus any indirect effects acting within this range). Additionally, when the correlation length of the fluid ξ is long (relative to the range of the solute−solvent intermolecular potential), the indirect density inhomogeneities will extend far beyond the local region and comprise the long-range component of the density inhomogeneity. Indeed, as the critical point of the solvent is approached and the correlation length diverges, the spatial integral of the long-range density enhancements will diverge,[12,49,51] while that of the local density enhancements will remain finite. (Again, a connection can be made to the Chialvo and Cummings partitioning,[47] as the indirect correlation function integral diverges while the direct correlation function integral remains finite as the critical point is approached. However, their direct term is formal and cannot be equated directly with the local density enhancement just defined.[50])

It is very important to recognize that different experiments probe the local and the long-range density inhomogeneities,[29,45−47] and that the range of an experimental probe determines to which effect such an experiment will be sensitive. The classic example of an experiment which is sensitive to local effects are solvatochromic shift experiments,[42,44] which detect changes in the solvation energy of a probe molecule as a result of changes in the local solvent density. The classic experimental probe of long-range density inhomogeneities are partial molar volume measurements,[52] which measure the change in the volume of a solution upon addition of solute.[31,47,49,53−59] Clearly, this latter experiment will be affected by changes in the average solvent density over long ranges (e.g. the container volume), while the former will only be sensitive to changes in the average solvent density which occur within the range of the solute−solvent interaction potential and can thus alter the energetics of solute solvation. Note that a probe of short-range structure will always be sensitive to local density inhomogeneities, yet be insensitive to the growing extent of the long-range fluctuations (except insofar as there is a relation between the presence of extended fluctuations and fluctuations in the local environment[10]). Similarly, a probe of the long-range structure will be sensitive to the growth of the extended correlations, becoming insensitive to the local density inhomogeneities as the correlations become long-range and begin to dominate.

Because in the compressible regime the origins of the local and the long-range density inhomogeneity effects differ, i.e. they are controlled by the direct and indirect mechanisms, respectively, the bulk density dependencies of these effects are not required to be the same. In fact, the magnitude of the long-range effect can be shown to diverge according to the divergence of the correlation length, such that its magnitude is directly tied to the compressibility κ.[47,49,51] As a result, for near-critical isotherms, the long-range density inhomogeneity is maximized at the critical density ρ_c. In contrast, local density enhancements are found to be maximized at bulk densities ranging roughly from $^1/_3\rho_c$ to $^1/_2\rho_c$.[45−47,60−62] Less is known about the behavior of local density depletions, which do not appear to be maximized at the same bulk densities as are local density enhance-

ments.[47,61] The early literature is confusing with regard to the bulk density dependence of local density enhancements, as it was generally assumed that the magnitude of the such enhancements should follow the compressibility. Additionally, the existence of two distinct effects was not appreciated, such that some analyses are muddled and the resultant conclusions are not precisely correct. In part because of the early confusion, the term "cluster", which has been used to refer to both local and long-range average density enhancements, was later rejected as a descriptor for the long-range enhancements.[45,63] This rejection arose in part because the term "cluster" was thought to imply the existence of stable physical aggregates, whereas the long-range enhancements represent only a statistical average over widely fluctuating densities,[49] i.e. it represents a correlation in the solvent density fluctuations over long range. As a result, use of the term cluster has more recently been restricted to the case of local density enhancements. Even in this case, however, use of the term "cluster" is going out of fashion, because, as will be seen in section IV, these local densities may also undergo large fluctuations[10,64] in some solute−solvent systems.

B. Attractive, Weakly Attractive, and Repulsive Solutes

As first proposed by Debenedetti and coworkers,[65−67] solutes in SCF solvents can be classified according to the type of density inhomogeneities they induce, both locally and over a long range. (For a review of formal relationships between local and long range density inhomogeneities, see ref 10.) Specifically, attractive solutes are those solutes which, in the SCF solvent of choice at the state point of interest, induce both a local density enhancement and an average long-range density enhancement. To emphasize the fact that the average long-range density enhancement does not imply the existence of a stable aggregate, we instead denote this long-range behavior by the corresponding partial molar volume change, which is negative. Weakly attractive solutes also induce a local density enhancement relative to the bulk value, but they induce a positive partial molar volume, implying an effective depletion of the average density over long range. Repulsive solutes induce both a local density depletion and a positive partial molar volume.

The formal definition of attractive, weakly attractive, and repulsive solutes can be made solely in terms of the solute−solvent direct correlation function integral.[65,67] Additionally, a working definition of these behaviors, which is not exactly equivalent to the formal definition, has also arisen. Formally, an attractive solute is defined to be one for which the solute−solvent direct correlation function integral is greater than one, i.e. $C_{12} > 1$,[65,67] where 1 represents the solvent and 2 the solute, and the correlation function integral is defined as ρ times the zero-frequency Fourier transform of the relevant direct correlation function,[51] here $c_{12}(r)$. To understand the physics of this formal definition of attractive solutes, it is useful to consider the behavior of the direct correlation function integral of the pure solvent, which is related to the compressibility by $C_{11} = 1 - (\kappa^{IG}/\kappa)$. As the critical point is approached and the compressibility diverges, C_{11} attains its maximal value, i.e. $C_{11} \rightarrow 1$. Thus, the condition for an attractive solute, $C_{12} > 1$, ensures that $C_{12} > C_{11}$. Note, however, that both direct correlation function integrals, C_{12} and C_{11}, vary with thermodynamic condition, such that the formal classification of the solute may vary with state point.[67] Additionally, the direct correlation function $c_{ij}(r)$ extends, approximately, over the range of the *ij* intereaction potential, and its integral remains finite as the compressibility diverges. This suggests that the direct correlation function integrals contain information about the local solvent density enhancements, although they should not be interpreted as representing local densities, ρ_l. The error of this physical interpretation becomes apparent in highly incompressible fluids, where the direct correlation function integral becomes large and negative.[51] However, because these integrals do contain *information* about the local density enhancements, the relation $C_{12} > C_{11}$ suggests that attractive solutes are those for which the local density enhancement around the solute, $\rho_{l,12}$, measured from experiment or computed from the total correlation function, is greater than the local density around a solvent molecule, $\rho_{l,11}$, and this local density criterion provides a working definition of attractive solutes, i.e. $\rho_{l,12} > \rho_{l,11}$. An additional important point here is that the average local density around a solvent molecule in a highly compressible SCF, $\rho_{l,11}$, may be greater than the bulk density of the fluid, ρ, such that the criterion $\rho_{l,12} > \rho$ is insufficient for determining attractive behavior.[10,15,68,69] That $\rho_{l,11}$ may be greater than ρ can be understood from Figure 1, in which it is clear that the majority of solvent atoms reside in the higher density regions, such that an average over the local solvent densities around solvent atoms yields an average local density $\rho_{l,11}$ which is greater than the bulk density ρ.[10,68]

A weakly attractive solute is formally defined as one for which $0 \leq C_{12} \leq 1$.[65,67] Since an ideal gas has an average local density equal to the bulk density and should thus have a direct correlation function integral of zero, this formal definition implies, loosely speaking, that a weakly attractive solute is one for which the average local density around the solute is less than that around a solvent molecule ($C_{12} < 1$), but is still in excess of the bulk density ($C_{12} > 0$). Thus $\rho_{l,11} \geq \rho_{l,12} \geq \rho$ provides a working definition of weakly attractive solutes. It follows that the average long-range density enhancements induced by the local perturbation will not be as strong around the solute as they are around a solvent molecule, and thus the transmutation of a solvent molecule to a solute molecule will cause a decrease in the average long-range density enhancement such that the volume of the solution will expand.[70] Finally, note that in practice attractive and weakly attractive solutes are often lumped together, such that any solute which has a surrounding average local density greater than the bulk value, i.e. $\rho_{l,12} < \rho$, is considered to be attractive.

Lastly, a repulsive solute is, formally, one for which $C_{12} < 0$,[65,67] suggesting that repulsive solutes may be approximately defined as those solutes around which the average local density is depleted compared to the bulk density, $\rho_{l,12} < \rho$. This phenomenon of depleted density has been referred to as cavitation. Although repulsive and weakly attractive solutes have both been observed experimentally and/or theoretically, by far the most frequently examined solutes are attractive.

C. Bulk Density Dependence of Local Density Inhomogeneities

The way in which local solvent density enhancements vary with the bulk solvent density at constant temperature, $T \gtrsim T_c$, is extremely important, because it provides the characteristic signature of such density inhomogeneities. As stated earlier, as pressure (P), and thus the bulk density, is increased, the relative local density $\tilde{\rho}_l = \rho_l/\rho$, where ρ_l and ρ are the local and bulk densities, respectively, is generally maximized at bulk densities between $^1/_2$ to $^1/_3$ of the critical density, ρ_c.[29,45−47,60−62] An alternative quantity that is sometimes considered is the excess local density, $\rho_l^{ex} = \rho_l - \rho$. This quantity is also usually maximized below the critical density, but it will reach its maximum at higher bulk densities than will the relative local density $\tilde{\rho}_l$. (Note that the *relative* excess local density $\tilde{\rho}_l^{ex} = \rho_l^{ex}/\rho$ differs from the relative local density $\tilde{\rho}_l$ only by a constant.) The local density itself, however, will increase continuously as the bulk density is increased. Hence, observation of local density enhancements, ρ_l, often relies on the fact that the local density changes at a different rate than the bulk density as the pressure, and thus the bulk density, is increased. Specifically, as the local density enhancement grows in at low pressures, the local density increases more rapidly than does the bulk density, and then, at increased pressures, the local density increases less rapidly than does the bulk density, as the bulk density catches up to the value already attained locally. At very low and very high bulk densities, the local and bulk densities increase at similar rates. These trends are illustrated in Figure 2, as a function of both pressure and bulk density. Note that the large compressibility near the critical point means that $\partial\rho/\partial P$ is extremely large. As a result, pressure-dependent studies always exhibit

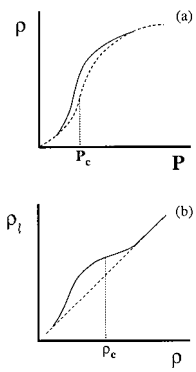

Figure 2. Typical behavior of the local density (solid line) and the bulk density (dashed line) on a near-critical isotherm as a function of (a) pressure and (b) bulk density.

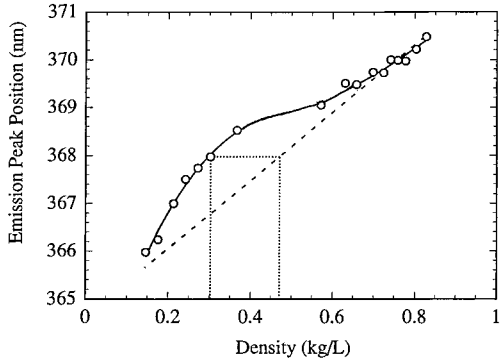

Figure 3. Fluorescence emission peak position as a function of bulk density for SC CO_2 at $T_r \approx 1.01$ (points). Solid line provides a guide to the eye. Dashed line is the bulk-density-based reference line, determined by extrapolation from the high-pressure results. Dotted line shows the usual method of estimating local densities, see text. (Data from ref 71.)

a rapid variation near the critical pressure P_c, Figure 2a. Much more information about the local density is therefore obtained when this derivative is removed and the experimental observable is expressed as a function of the bulk solvent density, Figure 2b.

Experimentally, solvent effects are typically examined by measuring properties of a probe solute molecule, e.g. a spectroscopic shift, which are sensitive to the local solvent environment. To evaluate local solvent densities, one needs to be able to express the measured property, M, as a function of some set of solvent properties, $\{\tilde{\epsilon}_s\}$, which can be related to the solvent density. An example of a commonly considered solvent property for such analyses is the dielectric constant, ϵ. If the dependence of the measured solute property on the solvent properties, $M\{\tilde{\epsilon}_s\}$, is known from liquid solvent studies, and the density dependence of these bulk solvent properties, $\{\tilde{\epsilon}_s(\rho)\}$, is known for the pure SCF of interest, then the bulk density dependence of the measured quantity, $M(\rho)$, can be predicted. The local density under various SC conditions can then be extracted by comparing the measured values of M, $M_{meas}(\rho)$, to the values predicted on the basis of the bulk density of the SC fluid under the experimental conditions, $M(\rho)$. If it is assumed that the measured values of M reflect the local density of the solvent around the solute, i.e. $M_{meas}(\rho) = M(\rho_l)$, then comparison of M_{meas} and $M(\rho)$ enables one to extract the local density ρ_l at each state point. As an example, consider a representative plot of the measured (M_{meas}) and predicted ($M(\rho)$) values, as shown in Figure 3. Here, spectral peak positions measured by Brennecke and co-workers[71] for the fluorescence emission of anthracene in SC CO_2 at a reduced temperature of $T_r = T/T_c \approx 1.01$ are shown for a range of reduced densities from $\rho_r = \rho/\rho_c \approx 0.3-1.8$. The dashed line represents the predicted values based on the bulk density ($M(\rho)$), while the points are the measured values ($M_{meas}(\rho)$). The deviation between the measured and predicted values signifies local density enhancements. To determine the effective local density ρ_l at, for example, a bulk density of 0.3 kg/L, one simply finds the bulk density at which the predicted value of $M(\rho)$ is equal to the observed value of M_{meas} at $\rho = 0.3$ kg/L, here 0.47

kg/L. Equating $M_{meas}(\rho) = M(\rho_l)$ then gives ρ_l as the bulk density just found, i.e. $\rho_l = 0.47$ kg/L. Notice that the shape of the curve in Figure 3 is qualitatively similar to the local vs bulk density shown in Figure 2, the only difference being that the bulk density based prediction, $M(\rho)$, is not necessarily a straight line (although it is so here). Figure 3 thus illustrates a complication of local density enhancement studies, which is that local densities cannot be extracted from experiment unless a curve predicting the expected behavior of the measured property on the basis of the bulk density is available. As a result, estimates of local density enhancements are only as good as the bulk density predictions on which they are based. Additionally, the existence and/or the magnitude of local density enhancements often cannot be inferred from studies in which the authors, because they were not explicitly looking for this behavior, did not supply a reference curve.

Because the behavior of the local solvent density with bulk density is relatively universal, i.e. it is qualitatively similar for all attractive solute−solvent systems, independent of the detailed molecular interactions, virtually all measured local solvent density dependent quantities exhibit the "three-regime" behavior exhibited in Figures 2 and 3. In particular, notice that at low bulk densities there is a rapid increase in M, followed by a region of relative invariance near the critical density, which is then followed by another region of increasing M. (A plot of M^{-1} would instead decrease at low and high density, but the characteristic invariance near ρ_c would remain.) Note that the near invariance in the middle region arises simply because the compressibility of the solvent enabled the formation of local density enhancements at lower densities, completing the local solvation in the first, or first few, solvent shells.[45,60,72,73] Subsequent changes in bulk density do not alter this local density significantly until the bulk density begins to exceed the local density. Indeed, the subsequent increase in the measured property is thought to arise from the compression of the local solvent sphere by the external fluid as liquidlike densities are achieved in the bulk fluid. While this characteristic behavior is apparent in a large number of the studies reviewed herein, the "three-regime" idea[60] and a demonstration of its universal appearance[74] were first put forward by Sun, Johnston, and Fox.

The density at which the maximum relative local density enhancement will occur will in general depend on a number of factors. Unfortunately, the specific dependence on any individual factor is unknown, as no detailed systematic studies have been performed with this goal in mind. Note that work along these lines is currently in progress.[75] One of the important factors is the spatial range over which the measured solute property is sensitive to the solvent density, as this defines the size of the local environment region in that particular measurement. Theoretical work on Lennard-Jones SCFs has shown that the location of the maximum local density enhancement shifts toward lower bulk densities as smaller local environment regions are considered when computing the local density.[13,46,47,61,64] Conversely, if the local region is taken to extend beyond the range of the solute−solvent intermolecular potential and include indirect density correlations, the maximum in the local density enhancement would shift toward the critical density ρ_c, or more rigorously, toward the density of maximum solvent compressibility on that isotherm. Another potentially important factor is the relative strengths of the solute−solvent and the solvent−solvent interaction potentials, i.e. the attractiveness of the solute being examined. For a more attractive solute, critical fluctuations are expected to be less important in the onset of solvent "clustering", such that solvent density enhancements may be maximized further from the critical point, i.e. at lower densities.[76,77] It should be remembered that an attractive solute will generally retain at least one or two nearest neighbor solvent molecules down to rather low bulk densities and that this behavior can lead to very large relative local densities, $\tilde{\rho}_l$, if only the first shell is included in the local density region, consequently shifting the maximum in the local density enhancement to lower bulk densities.[13] Lastly, the position of the maximal local density enhancement is expected to depend on temperature.

Note that the density enhancement effect will decrease as the temperature is raised further above the critical temperature, causing the characteristic three-regime behavior to vanish. The temperature to which observed local density enhancements persist will depend on the attractiveness of the solute−solvent system, the temperature to which high compressibility persists in the particular solvent (recall that as one moves away from the critical point universality ceases to apply, and some solvents may retain near critical behavior over a broader range of state points than others), and upon the definition of the local environment imposed by the measurement techniques. However, a rough rule of thumb is that (in three dimensions) local density enhancement effects are observed in the temperature range $T_r \leq 1.04$, whereas they may be reduced or nonexistent for $T_r > 1.06$, although exceptions do exist, with local density enhancement effects having been observed at temperatures higher than $T_r = 1.10$.[46,78−80] In particular, first shell density enhancements for strongly attractive solutes, such as multivalent ions in SC water, have been observed at much higher reduced temperatures.[77,81] Finally, the range over which compressibility-driven behavior will exist is dimensionality dependent, with two-dimensional fluids exhibiting critical behavior at higher reduced temperatures than do three-dimensional fluids.[10,12,82]

In addition to local density enhancement effects, many probe molecule properties M are sensitive to specific molecular interaction effects, most commonly hydrogen bonding. When these effects are present, they can substantially alter the bulk density dependence of M, complicating the analysis of local density enhancement effects. Additionally, there is now a substantial body of work, which is not reviewed herein, directed toward the characterization of hydrogen bonding and its effects under SC conditions.[25,33−41]

III. Evidence of Local Density Inhomogeneities

A. Static Measurements

1. Spectroscopic Measurements

a. Solvatochromic Shifts. *i. Kamlet−Taft π* Polarity Scale.* Some of the earliest evidence for local solvent density enhancements in SCF solvents came from studies correlating the pressure dependence of the UV-absorption maximum of a probe solute molecule in SCFs against the Kamlet−Taft π^* polarity scale.[83,84] This scale assumes the effect of solvent polarity on the spectral shift of the $\pi-\pi^*$ transition can be written as a product, $\delta\nu = s\pi^*$, of a solute-specific factor s, known for a given probe molecule, and a parameter π^* which accounts for the effect of the solvent polarity/polarizability. Yonker, Smith, and co-workers[83] extracted the π^* parameter from UV-absorbance studies of 2-nitroanisole in a series of low polarity SCF solvents at reduced temperatures of $T_r = 1.02$. Plots of the π^* values against reduced density exhibited a rapid rise at low densities, with a break in the slope to a much slower rise rate occurring at reduced densities of $\rho_r = 0.7 \pm 0.15$.

In subsequent studies, Yonker and Smith[84] used reaction-field solvation ideas to correlate the π^* values. Variations on this methodology have since been used frequently in the analysis of local density enhancements in SCFs. In this case, the authors computed the Onsager reaction-field factor for a nonpolar, polarizable medium, $f = 2\,(n^2 - 1)/(2n^2 + 1)$, where n is the index of refraction determined from a refractometric virial expansion based on the bulk densities of the pure SCF at each state point. Notice that the polarizability of a nonpolar solvent, and therefore f, will increase with density, as a result of the increased number of polarizable molecules per unit volume. On the basis of studies in liquids, it is expected that the Kamlet−Taft parameter π^* should vary linearly with the polarization factor f. Yonker and Smith[84] observed instead (Figure 4) two linear regimes of differing slope, at low and high polarization (which corresponds to low and high bulk densities). This break in slope was crudely interpreted as evidence of the onset of liquidlike behavior due to solvent clustering in the compressible regime.

ii. E_T Solvatochromic Scale. A solvatochromic scale, defined by the transition energy, E_T, of the absorbance maximum of phenol blue, was also used in some of the first studies to uncover local solvent density enhancement effects in SCFs. The shift in the transition energy of phenol blue with increased solvent polarity arises because the dipole moment of the excited state is 2.5 D greater than that of the ground state. This transition energy can be predicted according to Onsager reaction field based continuum solvation models, as is the Kamlet−Taft parameter π^*. For polar, polarizable fluids the theory of McRae[85] gives E_T in terms of the solvent's dielectric constant ϵ and its index of refraction n as

$$E_T = A\left(\frac{n^2-1}{2n^2+1}\right) + B\left(\frac{\epsilon-1}{\epsilon+2} - \frac{n^2-1}{n^2+2}\right) + C \quad (1)$$

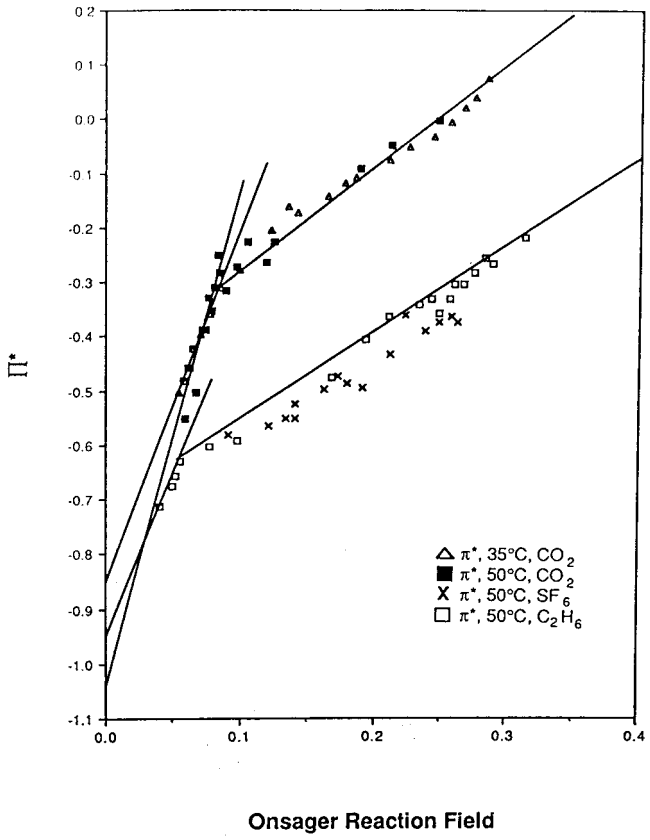

Figure 4. Plot of Kamlet−Taft π^* vs the polarization factor f for CO_2 at (open triangles) 35 °C ($T_r = 1.01$) and (filled squares) 50 °C ($T_r = 1.06$), and (crosses) SF_6 at 50 °C ($T_r \approx 1.01$) and (open squares) ethane at 50 °C ($T_r = 1.06$). (Reprinted from ref 84. Copyright 1988 American Chemical Society.)

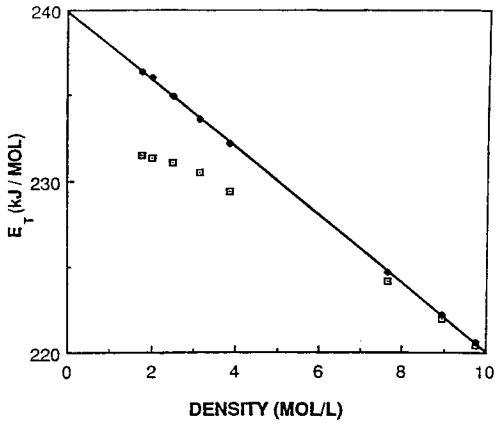

Figure 5. Transition energy for phenol blue vs density in 1,1-difluoroethane at 423 K ($T_r = 1.09$): open squares, observed values; diamonds, eq 1. (Reprinted from ref 8 with permission of the American Institute of Chemical Engineers. Copyright 1987 AIChE. All rights reserved.)

where the constants are known for phenol blue. Note that in nonpolar, polarizable solvents $\epsilon = n^2$, the second term becomes zero, and the first may be expressed as $(\epsilon - 1)/(2\epsilon + 1)$.

Johnston and co-workers[8,86,87] measured E_T values in both polar and nonpolar organic SCFs and compared the density dependence of these measured shifts with those predicted by the theory of McRae, Figure 5. Using the procedure outlined in section II, these authors extracted local solvent densities around

phenol blue in SC ethylene[86] and in SC 1,1-difluoroethane.[8] The SC ethylene study is probably the first study in which local densities were extracted from experimental measurements. Unfortunately, these authors attempted to correlate the observed local densities with the solvent's compressibility—a correlation with holds loosely but does not stand up under rigorous analysis, since, as stated in section II, the maximum in the local density enhancement does not coincide with the maximum in the compressibility, even though the local density enhancements are intimately connected with the compressibility of the fluid. These authors were not alone in attempting to make this connection (e.g. ref 84), and it was a number of years before this issue was put to rest.

Ikushima and co-workers[88] performed a similar analysis of the spectral shifts of *N*-phenoxide betaine dye ($E_T(30)$) in SC CO_2 at $T_r = 1.06$. However, these authors used a slightly different predictive equation for evaluating $E_T(30)$ of (ϵ, n) than did Johnston and co-workers. When compared to the predicted $E_T(30)$ values, the data clearly demonstrate the signature of local density enhancements illustrated in Figure 3.

Both Johnston and Ikushima and their respective co-workers used the E_T values, which provide a measure of the local density augmentation, to correlate reaction rates involving a reactant to transition state polarity change in SCF solvents, see ref 32. Note that the "cluster sizes" predicted by Ikushima et al. do not represent local density enhancements, as they were computed by using measured activation volumes in an expression[49] derived from consideration of the local *plus* long-range density correlations.

iii. EPR Shifts. The nitrogen hyperfine splitting constant also provides a sensitive probe of the local solvent polarity around a solute. Carlier and Randolph[45] used electron paramagnetic resonance (EPR) to examine the hyperfine constant of di-*tert*-butyl nitroxide in SC ethane at $T_r \approx 1.01$ (Figure 6a) and 1.08. Later, Ganapathy et al.[89] extended this work to SC CHF_3 and CO_2, obtaining much the same behavior as in the earlier work,[45] discussed below. The theory of McRae,[85] eq 1, becomes applicable to the hyperfine splitting constant given an appropriate choice of the constants *A*, *B*, and *C*. Carlier, Randolph, and co-workers thus used a comparison of the measured splitting constants with those predicted by this theory on the basis of the bulk solvent properties (as outlined in section II) to extract the bulk density dependence of the local density enhancements, Figure 6b.

Carlier and Randolph[45] observed (Figure 6b) that the maximum in the relative local density, $\tilde{\rho}_l = \tilde{\rho}_l/\rho$, occurred at a bulk solvent density of approximately $\rho_r \approx 0.5-0.6$ for the more near-critical temperature, whereas the compressibility of the fluid is maximized at $\rho_r \approx 0.95$ at this temperature. These authors surveyed the literature results available at that time (1993) for $\tilde{\rho}_l$ vs ρ and found that the maximum in $\tilde{\rho}_l$ occurred consistently at reduced densities between $^1/_2$ to $^1/_3$ of the critical density. Although this behavior was observed (and noted) in a few earlier works,[46,60,90]

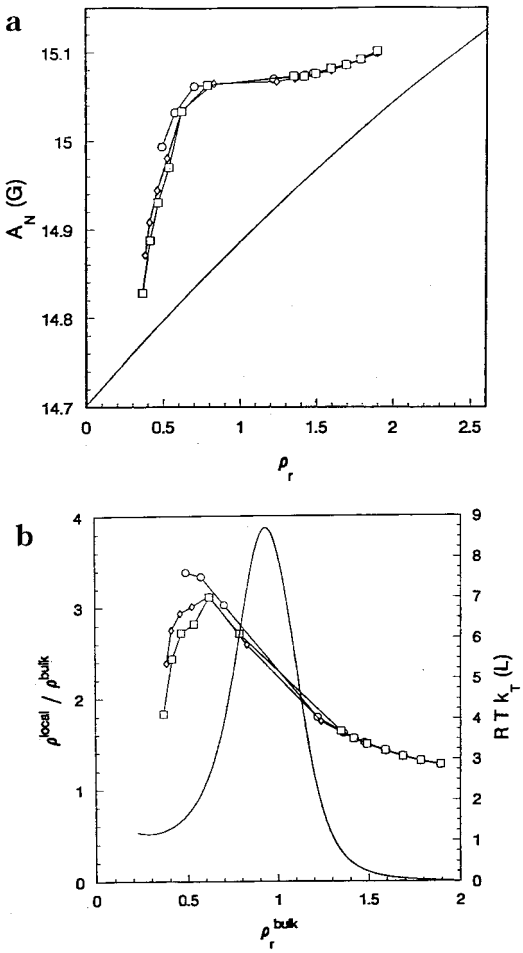

Figure 6. (a) Nitrogen hyperfine splitting constant vs the reduced bulk density ρ_r for DTBN in ethane at 308 K ($T_r \approx 1.01$). Symbols: observed values at different concentrations of DTBN; line: eq 1. (b) Relative local densities $\tilde{\rho}_l$, extracted from the hyperfine splitting constant data above, vs the reduced bulk density ρ_r. The isothermal compressibility of ethane at 308 K is presented for comparison (solid line). (Reprinted from ref 43 with permission of the American Institute of Chemical Engineers. Copyright 1993 AIChE. All rights reserved.)

the work of Carlier and Randolph provided the first definitive statement of this phenomena, along with the recognition that this behavior is quite general. Note that the early onset of the local solvent density augmentation is generally thought to reflect a filling of the inner solvation shells, as discussed in section II.

iv. UV Absorption. Numerous authors have examined solvatochromic shifts of UV−visible absorption spectral maxima of probe molecules in SCFs.[34,60,71,73,91−94] The systems considered include (dimethylamino)benzonitriles (DMABN), ethyl *p*-(*N*,*N*-dimethylamino)benzoate (DMAEB), 9-cyanoanthracene (9CA), pyrene and azulene in SC ethane, propane, CHF_3, and CO_2. In all cases, the solvent shifts vs reduced density exhibit the characteristic behavior shown in Figure 3, although in some cases either the rapid rise at low pressure or the transition to rapidly increasing behavior at high pressures is not observed, because the data covers an insufficient range of pressures. Sun et al.[60] present data which quite clearly covers all three regimes (Figure 7), and

these authors put forth the three-regime idea discussed in section II.C. In a few of the studies the data was analyzed by showing that the measured shifts exceed the linear dependence on the solvent's polarity factor expected on the basis of the theory of McRae.[73,91−93,95] While these works indicate a local density enhancement for densities below the critical density, the local densities were extracted (by the method outlined in section II) only in refs 73, 93, and 95. Rice et al.[95] observed that the local density enhancements around 9CA in both CO_2 and CHF_3 were both greater than, and shifted toward lower density than, the enhancements in ethane. This combination of behaviors is consistent with the idea that more attractive solute−solvent systems, e.g. 9CA in SC CO_2 and CHF_3, will have a maximum in the relative local density which is shifted to lower bulk density than in a less attractive system, e.g. 9CA in ethane. That 9CA−CO_2 acts more attractively than 9CA−ethane, a fact which is also borne out by the relative magnitude of the spectral shifts in these systems,[60] is most likely a result of the quadrupole moment of CO_2. That the solvating power of solvents having higher order multipoles, like CO_2, frequently exceed that predicted on the basis of their dielectric properties (ϵ and n) is known from liquid studies.[96] Kajimoto et al.[73] also determined local densities. These authors used an aggregation model based on Langmuir absorption equilibria to determine the number of solvent molecules in the first solvation shell of DMABN in SC CHF_3.

v. Fluorescence Emission. Fluorescence emission also shows solvatochromic behavior, and a number of studies have used emission spectral shifts to characterize local density enhancements in SCFs.[60,71,74,97−99] In all cases the bulk density dependence of the spectral shifts behaved as expected in the presence of local density enhancements.

Zhang et al.,[71] who examined the fluorescence emission of anthracene in SC CO_2, show the spectral shift as a function of bulk density, Figure 3. The local densities were extracted by comparison of the measured shifts with the best fit line through the high-pressure data where no local density augmentation is expected. The relative local density was found to peak at $\rho_r \approx 0.6$ at a value 1.75 times larger than the bulk density.

Heitz and Maroncelli[99] examined 1,3,6,8-tetraphenylpyrene (TPP) and 9,10-bis(phenylethynyl)anthracene (PEA), for which shifts in the absorption and emission peaks are comparable (i.e., a zero Stokes shift), in SC CO_2. The emission shifts were plotted against the reaction-field factor $(n^2 - 1)/(2n^2 + 1)$, eq 1, and compared to a linear regression of emission shifts in liquids against the same reaction-field factor. The extracted relative local densities, $\tilde{\rho}_l$, were found to be maximal at the lowest density considered, $\rho_r = 0.7$. Unfortunately, solubility limitations prevented the consideration of lower bulk densities.

Betts et al.[98] examined the Stokes shift, which is related to the difference between the spectral shifts of the absorption and emission bands, as a function of bulk density for 6-propionyl-2-(dimethylamine)-naphthalene (PRODAN) in N_2O. Over the density range considered, the Stokes shifts were roughly constant, within the noise. Comparison with predictions based on the relevant reaction-field factor yielded computed local density enhancements of up to 250%. Sun and Bunker[74] also examined PRODAN emission. These authors measured emission spectral shifts, rather than Stokes shifts, in SC CHF_3 and SC CO_2 and observed three-regime behavior in both cases. In these solvents, the turnover to low-density behavior was observed at a bulk density of $\rho_r \approx 0.75$, which is below the lowest density considered by Betts et al.,[98] explaining the absence of this turnover in Betts et al.'s data.

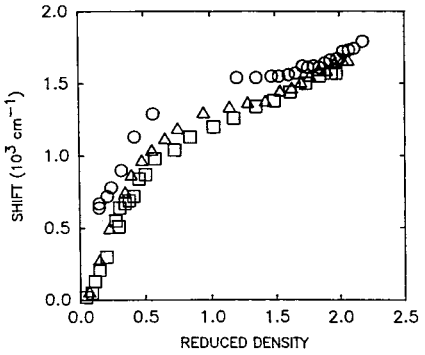

Figure 7. Solvatochromic shifts of the DMAEB absorption spectral maximum induced by changes in the reduced density of CHF_3 at (circles) 30 °C ($T_r \approx 1.01$), (triangles) 44.7 °C ($T_r = 1.06$), and (squares) 59.6 °C ($T_r = 1.11$). (Reprinted from ref 60. Copyright 1992 American Chemical Society.)

Sun et al.[60] compared absorption with fluorescence emission from the localized excited (LE) state bands for DMABN and DMAEB in SC CO_2. While both the absorption and LE emission band shifts exhibit the expected three-regime behavior as a function of bulk density, it was found that the absorbance shifts *exceeded* the emission shifts. The authors suggest that this is unexpected and that it points to variation in the solute geometries with solvent density.

vi. TICT Emission Shifts. Solvatochromic shifts can also be analyzed for the fluorescence emission of twisted intramolecular charge transfer (TICT) states. Both the spectral shift of the TICT band and the relative intensity of the TICT to localized state (LE) emission are sensitive to the local solvent environment. TICT emission spectral have been measured for the TICT-forming probes DEAEB,[74] DMAEB,[60] and DMABN[60,73] in SC CHF_3 and CO_2. Sun and co-workers[60,74] considered both TICT shifts and relative intensities as a function of the bulk density, and saw, in all cases, the expected rapid rise in the measured values at low density followed by a leveling off. Kajimoto and co-workers[73] observed a similar behavior for the intensity ratios. These latter authors also provide more rigorous evidence of density enhancements by showing that the TICT shift is not linear in the relevant reaction-field factor, but exhibits the usual local density dependent behavior, Figure 8. However, the effective local densities were not extracted.

vii. IR Shifts. The dependence of some vibrational mode frequencies on the surrounding solvent envi-

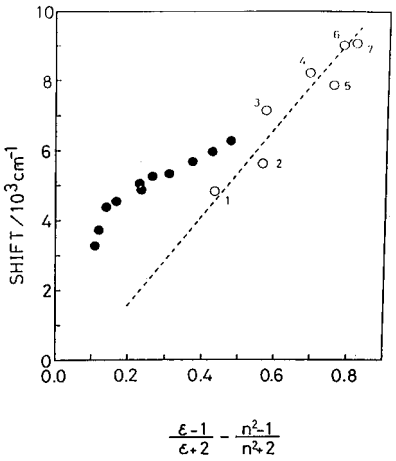

Figure 8. Solvatochromic shifts of the charge-transfer emission as a function of the solvent polarity factor. For the liquid-phase data (open circles), reasonable linearity was observed, whereas the data measured in supercritical CHF_3 at 50 °C ($T_r = 1.08$) (filled circles) deviate significantly. (Reprinted from ref 73. Copyright 1988 American Chemical Society.)

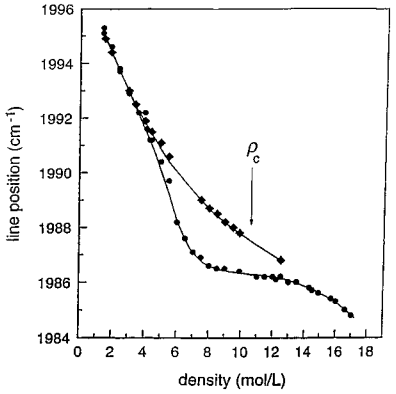

Figure 9. Infrared absorption line peak position of the T_{1u} asymmetric CO stretching mode of $W(CO)_6$ in CO_2 vs density at (circles) 33 °C ($T_r \approx 1.01$) and (diamonds) 50 °C ($T_r = 1.06$). Lines provide a visual aid and ρ_c marks the location of the critical density. (Reprinted with permission from ref 100. Copyright 1997 American Institute of Physics.)

ronment provides yet another tool for examining local density augmentation in SCFs. Infrared (IR) vibrational spectroscopy provides a complementary tool to the UV−visible methods just discussed, because very different probe molecules may be used in IR than in UV−visible spectroscopy. Despite this advantage, only a few IR spectral shift studies have been performed in SCFs, perhaps because the magnitudes of these shifts are usually small.

Fayer and co-workers[100,101] have presented very nice data for the T_{1u} asymmetric stretch of $W(CO)_6$ in SC CO_2 (Figure 9), ethane and CHF_3 and the symmetric stretch of $Rh(CO)_2acac$ in SC CO_2 and ethane. For these systems, the vibrational peak shifts to lower wavenumber with increasing solvent density. In all cases, for the $T_r \approx 1.01$ isotherm, the shifts exhibit a rapid decrease at low densities followed by a region of near invariance and a subsequent turnover to a more rapid decrease at higher densities, as shown in Figure 9. These data exhibit the classic behavior generally attributed to local density enhancements in the vicinity of the critical point, and although these authors do not invoke solvent density enhancements explicitly in their analysis, their hydrodynamic-based theory[102] does involve total and direct correlation function integrals, which implicitly contain local density information.

Ikawa and Fujita[103] examined the OH stretch frequencies of 4-hydroxy-4-methylpentan-2-one in SC Xe at $T_r = 1.03$ as a function of pressure. A plot of the frequency shift of the intramolecular hydrogen-bonded OH stretch against the polarity factor $(\epsilon - 1)/(2\epsilon + 1)$, eq 1, shows the expected linear decrease in wavenumber at low and high densities, with a deviation characteristic of local density enhancement effects at intermediate densities. One somewhat surprising aspect of this work, however, is that the maximum deviation from linear behavior occurs at a polarity factor of ~0.07, which, according to the authors, corresponds to a pressure *greater* than the critical pressure, i.e. $P_r \approx 1.2$. On the basis of the other studies reviewed herein, the maximum would be expected to occur at a density below the critical density, which for near-critical isotherms, would occur around the critical pressure, $P_r = 1$. However, at higher temperatures, higher pressures are required to obtain this same density, which could possibly explain the present result for $T_r = 1.03$.

b. Intensities. *i. Py Scale.* The intensity ratio, Py, of the first and third vibronic bands of the pyrene fluorescence emission spectrum is sensitive to the surrounding solvent polarity and polarizability, and has thus been used to examine local density enhancements in SCFs. In fact, Py values have been shown to have a linear relationship with the Kamlet−Taft parameter π^* [104] and can thus be linearly correlated with a reaction-field parameter. Py measurements have been used to show the universality of the three-regime behavior of compressible SCFs,[74] to extract local density enhancements[17,46,72,105] and to examine the local density augmentation around the excited state of pyrene, for comparison with the local density augmentation found around the ground state of pyrene.[93]

Sun and Bunker[74] examined Py values in SC CO_2 and CHF_3. These authors observed the classic three-regime behavior in both solvents. In fact, scaling of the Py data according to $(Py - Py^{gp})/(Py^c - Py^{gp})$, where Py^{gp} and Py^c are the Py values in the gas phase and at the critical density, respectively, allowed the reduced bulk density dependent data for SC CO_2 and for SC CHF_3 to be plotted on top of each other. These scaled Py curves are identical, except in the high-density, liquidlike regime where the rise of Py in CO_2 is more rapid than in CHF_3. Using similar scaling techniques, these authors were also able to demonstrate the universality of the three-regime behavior by overlaying the Py data with the density-dependent spectral shifts of PRODAN fluorescence emission in SC CO_2 and CHF_3 and of the TICT emission band of DEAEB in SC CHF_3 and ethane, Figure 10. Again, these curves lie roughly on top of each other, especially in the density-invariant region near and below the critical density. The greatest deviations between the different measurements are found in the high-pressure rises.

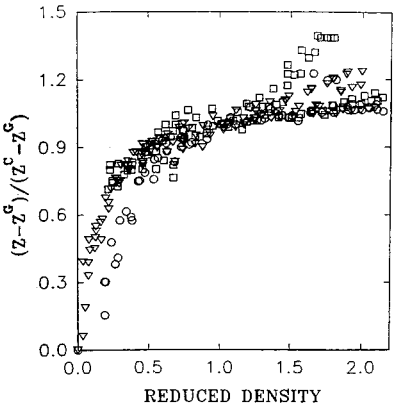

Figure 10. A global reduced scale plot for Py values (circles), solvatochromic shifts of the PRODAN fluorescence spectrum (squares), and solvatochromic shifts of the DEAEB TICT emission band and $\ln(x_{TICT}/x_{LE})$ (triangles), where x_{TICT} and x_{LE} are the fractional contributions of the TICT and locally excited state emissions, vs reduced density in supercritical CO_2, CHF_3, and ethane at different temperatures. (Reprinted with permission from ref 74. Copyright 1995 VCH Verlagsgesellschaft.)

Local density enhancements around pyrene have been extracted from Py data in SC CO_2, CHF_3, and ethane.[17,46,72,93,105] In a relatively early study, Brennecke et al.[105] extracted local densities by using linear fits to high-temperature Py data ($T_r = 1.06-1.1$) in the same solvents as reference curves. Plots of the extracted excess local density $\rho_l^{ex} = \rho_l - \rho$ vs reduced density showed the maximum in the excess density ρ_l^{ex} to occur, consistently, at slightly lower densities than do the maximum of the compressibilities. However, scatter in the data made it difficult for the authors to draw any definitive conclusions. Brennecke and co-workers[17] later repeated these studies and, using a linear extrapolation of high-pressure data as a reference line, extracted relative local densities $\tilde{\rho}_l = \rho_l/\rho$. In SC CO_2, these authors found $\tilde{\rho}_l$ to be maximized at $\rho_r \approx 0.7$ for $T_r = 1.01$ and at $\rho_r \approx 0.8$ for $T_r = 1.06$. Bright and co-workers[93] examined the same system at $T_r = 1.05$, and, by comparison with a reaction-field parameter based reference line, found the relative local density enhancement $\tilde{\rho}_l = \rho_l/\rho$ to be maximized at $\rho_r \approx 0.5$, Figure 11, a much lower value than found by Brennecke and co-workers.[17] Knutson et al.,[46] on the other hand, used high-temperature Py values ($T_r = 1.14$) to provide a reference line for the extraction of relative local densities for the same system, i.e. pyrene in SC CO_2 at $T_r = 1.05$. These authors found that at $\rho_r \approx 0.5$, the lowest density considered, the relative local density $\tilde{\rho}_l = \rho_l/\rho$ was still increasing with decreasing density, Figure 12, such that $\tilde{\rho}_l < 0.5$. This result, while in disagreement with both Brennecke's and Bright's studies, is consistent with the results of Sun et al.,[72] who, using a reaction-field parameter (which differed from that considered by Bright in ref 93) to create the reference line for their measured Py values, found ρ_l^{ex} in SC CO_2 at $T_r = 1.05$ to be maximized at a reduced density of $\rho_r \approx 0.35$. Note that these authors' consideration of the excess local density, ρ_l^{ex}, rather than the relative local density, $\tilde{\rho}_l$, considered by the other authors, should have

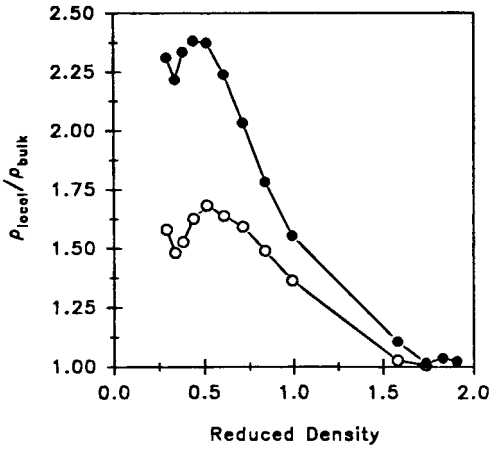

Figure 11. Comparison of relative local densities $\tilde{\rho}_l$ around pyrene in its ground state (open circles), extracted from electronic absorbance spectra, and in its excited state (filled circles), extracted from Py intensities, in CO_2 at 45 °C ($T_r = 1.05$). (Reprinted from ref 93. Copyright 1995 American Chemical Society.)

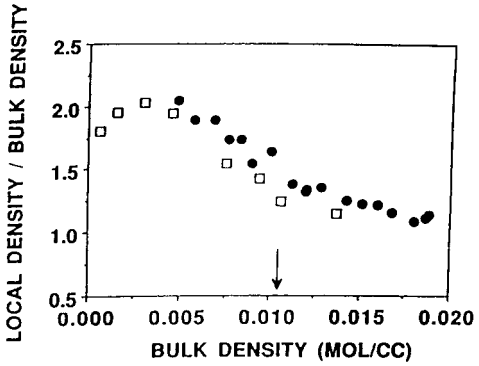

Figure 12. Comparison between relative local densities $\tilde{\rho}_l$ around pyrene in CO_2 at $T_r = 1.02$ deduced from Py intensities (solid circles) and molecular dynamics simulations (with Lennard-Jones potentials) using a cutoff radius of 1.94σ (open squares). The arrow denotes the critical density of CO_2. (Reprinted from ref 46. Copyright 1992 American Chemical Society.)

shifted the location of the maximum local density enhancement to *higher* bulk density, rather than to the lower density observed. Thus, there is little agreement in the results of these four studies, a result which most likely reflects the different choices of reference lines, and highlights the sensitivity of extracted local densities to this choice.[106] Additionally, when comparing results for the position of the local density enhancement maximum, it is important to remember that this position can be very sensitive to the exact quantity being considered, i.e. ρ_l^{ex} or $\tilde{\rho}_l$.

Since Py values represent relative emission intensities from excited-state pyrene, they probe the local solvent environment around the excited state, as it is assumed that solvent nuclear rearrangement to an equilibrium ground-state configuration does not occur on the emission time scale. Bright and co-workers[93] took advantage of this feature of Py values and compared the excited-state local densities computed from the Py intensities with ground-state local densities computed from pyrene absorbance shifts, which probe the ground-state local solvent environment. The results, Figure 11, show that the relative local

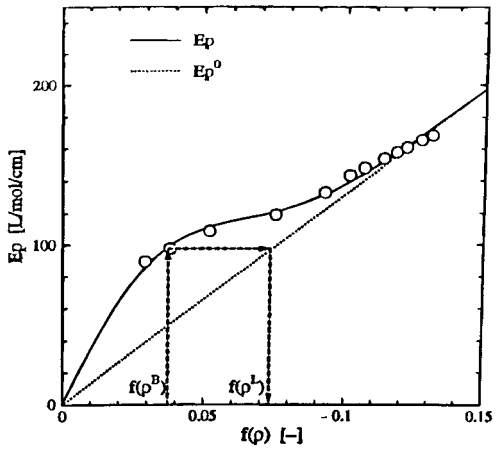

Figure 13. Infrared molar absorption coefficient (Ep) for the aromatic ring stretch of analine in CO_2 at 318.2 K (T_r = 1.05) (circles) vs the bulk density reaction-field factor $f(\rho)$ (see text). The solid line represents a two-parameter fit to the data, while the dotted line represents the expected linear dependence of the data on $f(\rho)$. (Reprinted from ref 108. Copyright 1997 American Chemical Society.)

densities around both the ground and excited states of pyrene were maximized at $\rho_r \approx 0.5$, but that the excited-state relative density enhancement at this point, $\tilde{\rho}_l \approx 2.5$, is about 50% greater than the relative density enhancement around the ground state. This result is consistent with semiempirical studies[107] which predict the CO_2−pyrene interaction to be more favorable for excited-state pyrene than for ground-state pyrene, and it illustrates the dependence of local density enhancements on the strength of the solvent−solute interactions.

ii. FTIR Absorption Intensities. Wada, Inomata, and co-workers[108] recently demonstrated that absorption intensities from Fourier transform infrared spectroscopy (FTIR) can be used to quantitatively extract local density enhancements around a solute. Specifically, this technique is based on the idea that measured molar absorption coefficients for each vibrational mode can be given in terms of the dipole moment associated with that solute mode, and that the solvent effect on the solute dipole moment can be expressed as a product of the reaction-field factor $(\epsilon - 1)/(2\epsilon + 1)$ and a mode-specific coefficient. The utility of the technique was demonstrated on substituted benzene derivatives in SC CO_2 at $T_r = 1.05$, Figure 13.

2. Theoretical and Computational Studies

a. Theory. The important distinction between direct (local) and indirect (long-range) density inhomogeneity effects, defined in section II, was not immediately recognized. And, while it was gradually accepted that spectroscopic techniques were probing a shorter length scale phenomena than were partial molar volume experiments in the vicinity of the critical point, the development of a formal partitioning[47,109−111] of thermodynamic observables into nondivergent and divergent components underscored the importance of this distinction. Note that a more formal, detailed review of this partitioning than is provided below can be found in ref 10.

Chialvo and Cummings' [47] partitioning is based on the fact that the total solvent(1)−solute(2) correlation function $(g_{12}(r) - 1)$, which is related to the probability of finding a solvent molecule a distance r away from a solute molecule, can be separated into direct, $c_{12}(r)$, and indirect, $i_{12}(r) = g_{12}(r) - 1 - c_{12}(r)$, components according to the Ornstein−Zernike theory. The solvent−solvent total correlation function, $g_{11}(r)$, can be similarly decomposed. Chialvo and Cummings showed that the infinite-dilution partial molar volume of a solute, which is directly related to the average solvent enhancement or depletion around the solute, can be decomposed into a direct term which is expressed entirely in terms of the direct correlation function integrals C_{12} and C_{11} (defined in section II) and an indirect term which is expressed in terms of the corresponding indirect correlation function integrals, I_{12} and I_{11}. The direct component of the partial molar volume, will, like the direct correlation function integrals, remain finite as the critical point is approached and the compressibility diverges ($\kappa \rightarrow \infty$). In contrast, the indirect component of the partial molar volume, like the indirect correlation function integrals, will diverge as does the compressibility, κ. Thus, as the critical point is approached, the divergent, indirect component of the partial molar volume will dominate, which suggests that partial molar volume measurements near the critical point reflect indirect density inhomogeneities (see section II.A) and should track the diverging compressibility, as they are observed to do.[47]

In contrast to the divergent component, the nondivergent, direct component may be maximized at densities below the critical densities, as was demonstrated by Chialvo and Cummings[47] for a Lennard-Jones solute−solvent system. This result is suggestive of a relationship between the nondivergent component of the partial molar volume and the local density enhancements measured spectroscopically. Such a relationship is also implied by the fact that solute solvation energies,[112] which are frequently the defining factor in spectroscopic measurements of solvent effects, can also be written in terms of the nondivergent, direct correlation function integrals.

One of the physical insights that is suggested by this formal treatment of the partial molar volume is the idea that in the vicinity of the critical point where the correlation length ξ is long, the local density enhancement (or depletion) arises from a direct interaction of the solute with the compressible solvent, whereas the long-range, divergent density enhancement (or depletion) arises from indirect solute−solvent interactions, i.e. from the solvent response to the presence of the local solvent density fluctuation induced directly by the solute. These are exactly the distinctions described in section II. However, as cautioned there, the formal partitioning into direct and indirect correlation function integrals cannot be mapped directly onto the physical idea of local and long-range density enhancements, or of direct and indirect density enhancements; note that ref 10 errs in this regard.

b. Simulation and Integral Equation Studies. *i. Distribution Functions: Lennard-Jones Solutions.*

Both computer simulation (Monte Carlo and molecular dynamics) and integral equation studies provide a means of observing local densities directly, through the solute−solvent radial distribution function $g_{12}(r)$. The normalization of this function is such that

$$\rho\int_0^R [g_{12}(r) - 1]\, d\mathbf{r} = N^{ex}(R) \qquad (2)$$

where $N^{ex}(R)$ is the average number of solvent molecules, within a distance R of the solute, in excess of the number expected in that volume on the basis of the bulk density. In early work, Wu, Lee, and Cochran[15,69] examined this excess number around both attractive and repulsive Lennard-Jones solutes in a Lennard-Jones solvent. Indeed, they found that the excess number $N^{ex}(R)$ rises rapidly, increasing to ∼100 molecules over a distance of about 10 molecular diameters for the attractive case, whereas it decreases to a value of about −6 over the same distance for the repulsive case. Note that the excess number incorporates both direct and indirect components of the density enhancement (depletion), and that there is no precise distance at which one effect ends and the other begins.

Numerous authors have examined the effect of thermodynamic condition on the local density enhancements evident in the solute−solvent radial distribution function.[15,67,113−116] In general, for attractive solutes, the nearest neighbor peak in the solute−solvent radial distribution function exceeds the nearest neighbor peak in the solvent−solvent radial distribution function, and this solvent enhancement in the first solvation shell around the solute is increased at more near-critical SC conditions. Additionally, it was demonstrated in one case that this peak-height difference of 35% under SC conditions ($T_r = 1.03$) nearly vanished under liquid conditions.[114]

An interesting feature of the formal definition of attractive, weakly attractive, and repulsive solute−solvent systems (see section II), which is based on the direct correlation function integral C_{12}, is that the behavior of a given solute−solvent system depends on thermodynamic condition. Petsche and Debenedetti[67] mapped out the state points under which attractive, weakly attractive and repulsive behavior will be observed for a hard core plus r^{-6} potential representation of naphthalene in SC CO_2. Within the range $1 \geq T_r \geq 2$ and $0 \leq \rho_r \leq 2$, all three behaviors were observed, with attractive behavior occurring in the most near critical region, and repulsive behavior occurring at the higher densities. While attractive/repulsive behavior is, strictly speaking, thermodynamic-condition-dependent, this dependence is usually ignored in the literature, where only approximate classification schemes are generally applied.

Another area of interest is the effect of the solute−solvent interaction potential, manifest in the solute−solvent Lennard-Jones parameters, on attractive/repulsive behavior, and, concomitantly, on the observed local density enhancements. Of particular note is the fact, proved by Debenedetti and Mohamed[65] and illustrated by Petsche and Debenedetti[113] for the Xe/Ne system, that if a dilute mixture of solute A in SC B behaves attractively, then a dilute mixture of solute B in SC A will behave repulsively! This behavior arises quite simply in a system where the AB interactions can be related to the AA and BB interactions by simple combining rules. In such cases, if the AA interaction is more favorable than the BB interactions, the AB interaction will be *more* favorable than the BB interaction, causing dilute A in SC B to behave attractively, but it (the AB interaction) will be *less* favorable than the AA interaction, causing dilute B in SC A to behave repulsively.

A number of authors also examined the effects of changing the individual Lennard-Jones parameters, i.e. the well depth ϵ and the molecular diameter σ, on the extent of attractive behavior, measured either by examining the direct correlation function integrals (formal definition) or by computing the average local density out to some arbitrary distance (working definition), i.e.

$$\rho_l(R) = \frac{N(R)}{[(4\pi)/3](R^3 - R_u{}^3)} \qquad (3)$$

where the number of local solvent molecules is

$$N(R) = \rho\int_0^R g_{12}(r)\, d\mathbf{r} \qquad (4)$$

and $[(4\pi)/3](R^3 - R_u{}^3)$ is the volume of the local region minus the volume taken up by the solute, with R_u usually taken to be $(^1/_2)\sigma_2$. In all cases it was found that attractive behavior is enhanced as the solute−solvent well depth is increased relative to the solvent−solvent well depth, corresponding to an increase in the ratio $\epsilon_{12}/\epsilon_{11}$ (2 = solute, 1 = solvent) when combining rules are used for the intermolecular interactions.[67,115,117] The effect of solute diameter, however, is less straightforward. Petsche and Debenedetti[67] show, for the hard core plus r^{-6} potential, that only a limited range of relative solute−solvent diameters will give rise to attractive behavior. For example, on a near-critical isotherm these authors found only size ratios of approximately $1 < \sigma_{12}/\sigma_{11} < 1.4$ exhibited attractive behavior. Hence, increasing the solute size may enhance attractive behavior, yielding greater local density enhancements, as observed by Liew, Inomata, and Saito,[117] or diminish the attractive behavior, yielding smaller local density enhancements, as observed by Zeng and co-workers.[115,116] Note that all of these studies used different methods for analyzing the local density enhancement effects—Petsche and Debenedetti used the correlation function integral C_{12}, Liew et al. used the average number of solvent molecules found to be bound strongly to the solute molecule on the basis of these solvent molecules' exchange rate, whereas Zeng and co-workers simply integrated the solute−solvent radial distribution function out to the position of the first minimum.

ii. Distribution Functions: Aqueous Solutions. Local density inhomogeneities around ions and neutrals in SC water have also been examined under various thermodynamic conditions via molecular dynamics simulation. The simple point charge model of water, which has critical parameters of $T_c = 578$ K and ρ_c

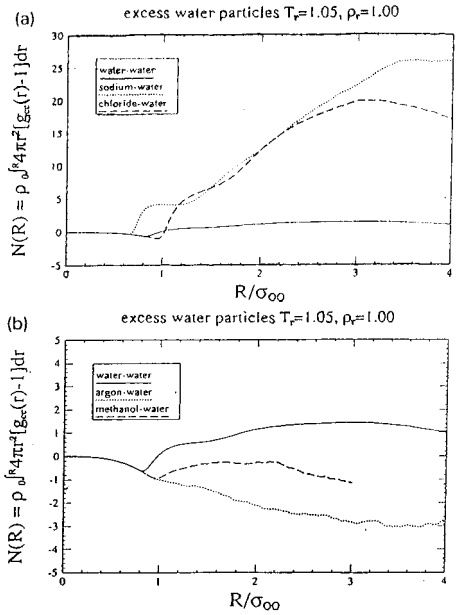

Figure 14. Average number of excess water molecules found, via molecular dynamics simulation, (a) surrounding a central water, sodium, and chloride particle, and (b) surrounding a central water, argon, and methanol particle, at $T_r = 1.05$ and $\rho_r = 1.00$ (state 2). (Reprinted from ref 118, copyright 1992, with permission from Elsevier Science Publishers.)

$= 0.27$ g cm^{-3} compared to values of $T_c = 647$ K and $\rho_c = 0.32$ g cm^{-3} for real water, has been used almost exclusively. Cummings, Cochran and co-workers[36,111,118,119] examined the excess number of water molecules (eq 2) as a function of distance around a variety of solutes at two state points: (1) $T_r = 1.0$ and $\rho_r = 1.5$ and (2) $T_r = 1.05$ and $\rho_r = 1.0$. The ions Na^+ and Cl^- [111,118,119] were found to induce significant density enhancements at both state points (Figure 14), with the enhancements being somewhat greater for the lower density state point,[119] e.g. at a distance of 3σ ($\sigma = 3.166$ Å), $N^{ex}_{Na^+} \approx 14$ for state point 1[120] and ≈22 for state point 2. The enhancements were also slightly greater around Na^+ than around Cl^-, e.g. at 3σ for state point 2, $N^{ex}_{Na^+} \approx 22$ while $N^{ex}_{Cl^-} \approx 20$, Figure 14. (Note that herein we quote N^{ex} relative to the bulk solvent density in each case, even where the original work used a different baseline.) An important note is that these authors observed a decrease in N^{ex} at large distances from the ions, indicating a depletion in solvent density relative to the bulk value, as a result of the finite number of molecules in the NVT simulation cell. This artificial depletion of density at long-range induces an effective pressure on the solute-induced local density enhancement, tending to reduce its size.[121]

The neutral solutes Ar (Figure 14),[36,118,119] benzene,[36] and toluene[36] were found to behave repulsively at both state points, meaning that they exhibit no first peak in the solute−water−oxygen radial distribution function, and that there is a net depletion of solvent molecules around these solutes over longer range, e.g. at state point 1 $N^{ex}_{benzene} \approx -14$ at 3σ while for Ar, this depletion is only $N^{ex}_{Ar} \approx -5$ at 3σ.[36] In contrast to the ions discussed above, the density inhomogeneity for these repulsive neutrals is more pronounced at the higher density state point, e.g. $N^{ex}_{benzene} \approx -7$ at state point 2 compared to $N^{ex}_{benzene} \approx -14$ at the higher density state point 1.[36,119,122] These results are consistent with Petsche and Debenedetti's conclusion for van der Waals systems that repulsive behavior is enhanced at higher densities.[67]

Methanol[118] (Figure 14) and Xe[36] were found to behave in a weakly attractive manner, in that they exhibit a first peak in the solute−solvent radial distribution function (at $\sim 1\sigma$), but exhibit a net depletion over longer range, e.g. at 3σ for state point 2 $N^{ex}_{Xe} \approx -2$. Methanol behavior was found to be very state point dependent, exhibiting very little long-range depletion at the lower density state point (Figure 14), but a depletion of -5 at the higher density, lower temperature state point. Similarly, benzonitrile[36] exhibits a first peak in the solute−solvent radial distribution function for the lower density state point, but not for the higher density state point, yet it exhibits long-range depletion in both cases. Thus benzonitrile switches from weakly attractive to repulsive behavior as the density increases,[36] again consistent with Petsche and Debenedetti's prediction. Pulitzer and co-workers used equation of state estimates of the direct correlation function integral combined with constant pressure computer simulations to determine that O_2 is weakly attractive in SC water at very low densities (<0.1 g cm^{-3}) and a high temperature of $T = 850$ K.[123]

Cui and Harris[81] provide additional density and temperature dependencies for the ionic solutes. These authors examined excess solvent numbers around Na^+, Cl^-, and the NaCl ion pair for temperatures ranging from 700 to 1000 K at densities of $\rho = 0.3$ g cm^{-3} ($\rho_r \approx 1.1$) and $\rho = 0.7$ g cm^{-3} ($\rho_r \approx 2.6$). For all of the solutes, these authors found the excess number to be greatest at the lower density and at the lowest temperature ($T_r \approx 1.2$ for SPC water). Note that even though this lowest temperature exceeds the critical temperature by a full 20%, these authors observed N^{ex} values around Cl^- of 5 and 12, in the first shell and within 10 Å, respectively. These N^{ex} values, while dropping to 3 and 6, are still nonzero at 1000 K, i.e. at $T_r \approx 1.7$. The excess number around the ion pair was found to be comparable to those around the individual ions in the first shell, but to be 30% smaller than around the ions in the 10 Å sphere, presumably because the ion pair appears neutral at longer range.

Flanagin et al.[80] showed that the density enhancements around the reactive solute $Cl^-\cdots CH_3Cl$, as measured by peak heights in the chloride−water-oxygen radial distribution function, decrease dramatically as the complex reacts and the charge on the chlorine becomes dispersed over the complex. In a similar vein, Re and Laria[124] showed that, at $T_r = 1.1$ and $\rho_r \approx 1.1$, the strong first peak around the Cl^- ion in the chloride−water-oxygen radial distribution function, which is about 7 times the bulk density, nearly vanishes around a neutral Cl atom, Figure 15b. Additionally, at a high, liquidlike density of 1 g cm^{-3} (still with $T_r = 1.1$), the peak around the Cl^- ion, which now has a height of only ~3 times the bulk

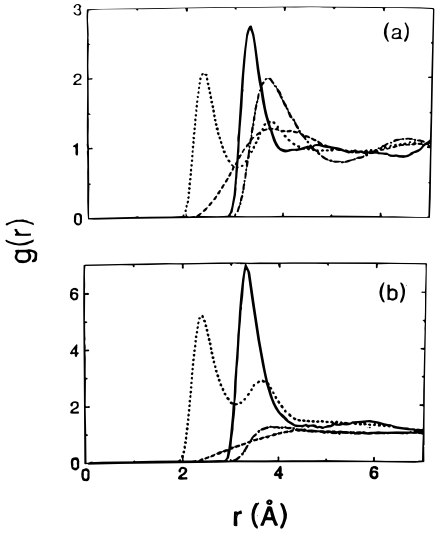

Figure 15. Equilibrium solute−solvent radial distribution functions (rdf) for supercritical water at 645.15 K ($T_r \approx 1.10$) and different densities: (a) $\rho = 1$ g cm^{-1} ($\rho_r \approx 3.7$) (b) $\rho = 0.3$ g cm^{-1} ($\rho_r \approx 1.1$); Cl^-−O rdf (solid line), Cl−O rdf (dash−dotted line); Cl^-−H rdf (dotted line), Cl−H rdf (dashed line). (Reprinted from ref 124. Copyright 1997 American Chemical Society.)

density, drops only by 50%, to ∼2, for a neutral Cl atom, Figure 15a. Clearly, at the more compressible conditions the solute−solvent interaction strength has a much greater influence on the local solvent environment than it does at higher, less compressible densities.

iii. Distribution Functions: Pure SCFs. Average local density enhancements are not just the province of SCF solutions, but may be observed in pure SCFs as well. Using the working definition of solute−solvent attractiveness (section II), one finds that a tagged solvent molecule falls exactly at the border between attractive and weakly attractive behavior, because the average local density around the tagged solvent is clearly the same as that around any other solvent molecule. Solvent-centered local density enhancements are a result of solvent "aggregation" (cf., Figure 1), which is simply a manifestation of the expected correlated density fluctuations near the critical point. Using the formal definition of solute−solvent attractive/repulsive behavior, on the other hand, one finds that a tagged solvent molecule (2) has $C_{12} = 1 - (1/\tilde{\kappa})$, where $\tilde{\kappa}$ is the reduced compressibility relative to that for an ideal gas, such that at the critical point, where $\tilde{\kappa} \rightarrow \infty$, $C_{12} = 1$, and the pure solvent system indeed falls at the border of attractive and weakly attractive behavior. Elsewhere in the compressible regime, where $\tilde{\kappa} > 1$, $0 < C_{12} < 1$, such that a pure SCF is, formally, weakly attractive in this regime. Note that the partial molar volume for the addition of a solvent molecule is always $1/\rho$, which is greater than zero (such that the fluid will expand), as is expected for a weakly attractive solute.

The expected *local* density enhancements around a tagged solvent molecule in pure SCFs has been observed in a number of studies. Gao's observation[125] of instantaneous solvent aggregation in SC water is reflected in the solvent-centered excess number of $N^{ex} \approx 1.5$ observed at a distance of 3σ in SC water at $T_r = 1.05$ and $\rho_r = 1.0$ by Cochran et al.,[118] Figure 14. In pure three-dimensional Lennard-Jones systems, Wu et al.[15,69] observed the solvent-centered excess number N^{ex} to reach a value of 8 by 10σ, whereas this value is only ∼2 locally, here defined as 3σ. Tucker and Maddox[10] showed explicitly for a pure two-dimensional Lennard-Jones system that the mean density around a solvent molecule (Figure 16), defined within a radius of 3.09σ, shifts to densities higher than the bulk value as the temperature is lowered toward the critical value, i.e. $T \rightarrow T_c^+$. These authors explained this phenomena by noting that as density inhomogeneities, i.e. correlated density fluctuations, appear on a length scale ξ (see Figure 1), one finds that by necessity there are many more atoms residing in high-density regions than in low-density regions. As a result, an atom will sample high-density environments much more frequently than it will sample low-density environments, causing the *average* local density to shift toward higher than bulk densities.[10,68]

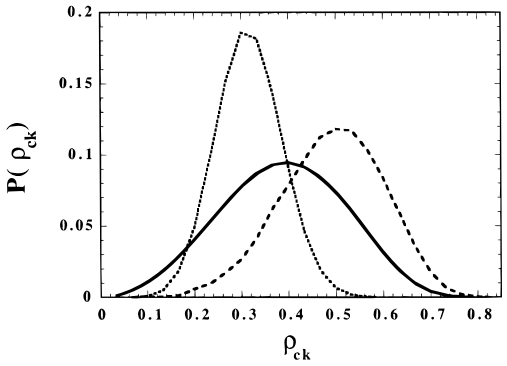

Figure 16. Distribution of local densities around a tagged solvent atom in a two-dimensional Lennard-Jones supercritical fluid at a reduced density $\rho_r \approx 0.86$ and reduced temperature $T_r \approx 1.17$ (solid line) and $T_r \approx 10.6$ (dotted line). Dashed line is the distribution around an attractive solute at $\rho_r \approx 0.86$ and $T_r \approx 1.17$. (Reprinted from ref 10. Copyright 1997 American Chemical Society.)

iv. Bulk Density Dependence of Local Densities. A number of simulation studies have examined the relative local solvent density, $\tilde{\rho}_l = \rho_l/\rho$, around solutes as a function of bulk density. We can thus begin to correlate the location of the maximum in this function ($\tilde{\rho}_l(\rho_r)$) with such parameters as the solute's attractiveness, the cutoff distance used in determining $\tilde{\rho}_l$ (see eq 3), and the temperature. We consider the function $\tilde{\rho}_l$ vs ρ_r first for attractive solutes and then for repulsive solutes.

1. ATTRACTIVE SOLUTES. We compare six studies[46,47,61,62,89,126,127] of $\tilde{\rho}_l$ vs ρ_r for attractive Lennard-Jones solute (2)−solvent (1) systems having $\epsilon_{12}/\epsilon_{11}$ in the range 1.45−1.72 and σ_{12}/σ_{11} in the range 1.23−1.44. We examine first the dependence upon cutoff distance and then upon temperature and the potential parameters. The temperature dependences in attractive ion−water systems are presented in this section as well. Finally, comparisons between the simulated bulk density dependencies of $\tilde{\rho}_l$ and those extracted from experiment are discussed.

Within the range of Lennard-Jones parameters considered, the most important feature in determining the location and magnitude of the maximum

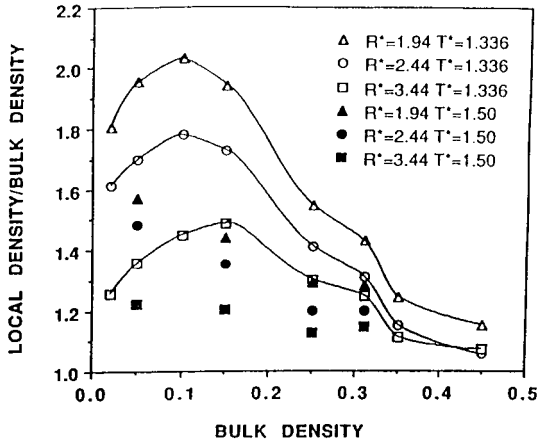

Figure 17. Relative local densities $\tilde{\rho}_l$ vs bulk density for Lennard-Jones pyrene in CO_2, computed from molecular dynamics simulation using different radial cutoffs (eqs 3 and 4) at two temperatures. All quantities in Lennard-Jones units; $T^* = 1.336$ corresponds to $T_r = 1.02$ and $T^* = 1.50$ to $T_r = 1.145$. (Reprinted from ref 46. Copyright 1992 American Chemical Society.)

relative local density on a near-critical isotherm is found to be the cutoff distance R used to define the local region, see eqs 3 and 4. In particular, when the cutoff distance R is increased, such that a larger region is used to evaluate the local density, the position of the maximum in $\tilde{\rho}_l(\rho_r)$ shifts toward higher densities, i.e. toward the critical density (Figure 17).[46,61] For example, when the cutoff R is taken at the first minimum in the solute−solvent radial distribution function $g_{12}(r)$, i.e. after the first solvation shell, the maximum in $\tilde{\rho}_l$ was found in all studies (except ref 47)[127] to occur at ρ_r less than or around 0.3. When the cutoff is extended to the second maximum in $g_{12}(r)$, the maximum in $\tilde{\rho}_l$ is found to fall in the range $\rho_r \approx 0.3-0.6$, while when the third peak is included, values of $\rho_r \approx 0.5-0.65$ are obtained.[46,61] (Note that in refs 62 and 89, $\tilde{\rho}_l(\rho_r)$ was found to be extremely flat for low values of ρ_r, such that at the first, second and third solvent shell cutoffs, respectively, $\tilde{\rho}_l$ is flat for values of ρ_r less that 0.3, 0.5, and 0.5.) This shift in the location of the maximum in $\tilde{\rho}_l$ with increasing cutoff distance R has also been observed around solvent molecules in a pure (two-dimensional) Lennard-Jones SCF.[64] The observed behavior is sensible, because, as the cutoff radius is increased, the integral over $g_{12}(r)$ (eq 4) picks up more contributions from the longer range, indirect average density enhancements which diverge at the critical density ($\rho_r = 1$). Thus, as the indirect enhancements play an increasingly important role, the maximum in the relative local density enhancement should shift toward the critical density, as is observed. Note that at very low densities first shell enhancements are generally still observed, due to the solute−solvent attraction.[10,13,62,64] This behavior has also been noted for ions in SC water.[76,128]

It is also observed that the maximum local density enhancement attained decreases with increasing cutoff radius R. Thus, for the first, second, and third shell cutoffs, maximum enhancements of ∼60−100%, ∼30−80%, and ∼25−50%, were found, respectively. This behavior is also reasonable, because mean solvent enhancements decrease with increasing distance from the solute, as evidenced by the decay envelope of the solute−solvent radial distribution function. Indeed, this decrease represents loss of the correlation of solvent density fluctuations with solute position as one moves away from the solute.

Temperature, which controls the proximity to the critical point, might also be expected to affect the behavior of the relative local densities, $\tilde{\rho}_l$ vs ρ_r. Further comparison of the above studies,[46,61,62,89] which were conducted on $T_r = 1.01$, 1.02, 1.07, 1.08, and 1.15 isotherms, show that temperature effects may not be as strong as expected, at least for such Lennard-Jones systems. First, the location of the maximum in $\tilde{\rho}_l(\rho_r)$, which correlates strongly with the cutoff distance R, appears to be insensitive to temperature. Second, substantial density enhancements of up to 56% and 10% for the first and second shell cutoffs, respectively, are observed at $\rho_r = 0.16$ for the highest temperature considered, $T_r = 1.15$. And, while the magnitude of the maximum value of $\tilde{\rho}_l$ decreases with increasing temperature, from >100% at $T_r = 1.02$ to ∼60% at $T_r = 1.08$ for the first shell cutoff and from 50% to ∼25% for the third shell cutoff, the higher temperature studies were conducted on the less attractive solute−solvent systems ($\epsilon_{12}/\epsilon_{11} \approx 1.5$ vs ≈ 1.7), such that the reduced potential interaction could account for some or all of the observed reductions of the density enhancement with temperature. Additionally, the radius ratio σ_{12}/σ_{11}, which can alter the degree of attractive behavior,[67] also varies between studies. For example, Munoz and Chimowitz[126] considered a system with a large energy ratio, $\epsilon_{12}/\epsilon_{11} = 1.7$, but a smaller size ratio, $\sigma_{12}/\sigma_{11} = 1.2$, and found a large, third shell cutoff enhancement of ∼70% at $T_r \approx 1.01$. Clearly, all of these factors affect the magnitude of the enhancement, and, as a result, neither the temperature dependence nor the potential-function dependence of the behavior of $\tilde{\rho}_l(\rho_r)$ with ρ_r could be unequivocally isolated from these studies.

However, dependence of the bulk density dependence of the local excess number of solvent molecules $N^{ex}(R)$, which is simply related to the relative local density $\tilde{\rho}_l(\rho_r)$, has been studied for an ionic system in SC water by Flanagin et al.[80] Note that when computing $N^{ex}(R)$, these authors subtract off the volume taken up by the solute, i.e. they use the radius of the solute, R_u, instead of 0 as the lower limit in eq 2. Using a two-solvent-shell cutoff located at the second minimum in the solute−solvent radial distribution function, these authors observed an excess of solvent molecules for all temperatures considered, from $T_r = 1.0$ to $T_r = 1.3$. The corresponding maximum N^{ex} values were found to range from 14 to 8 at $T_r = 1.0$ and 1.3, respectively. This persistence of density enhancements at high temperatures is consistent with the results of Cui and Harris,[81] Wood,[128] and Fulton and co-workers.[77] One might speculate that the existence of density enhancements at such high temperatures is a result of the strong, long-range Coulombic solute−solvent interactions, which could presumably induce compression in a solvent having only a modest compress-

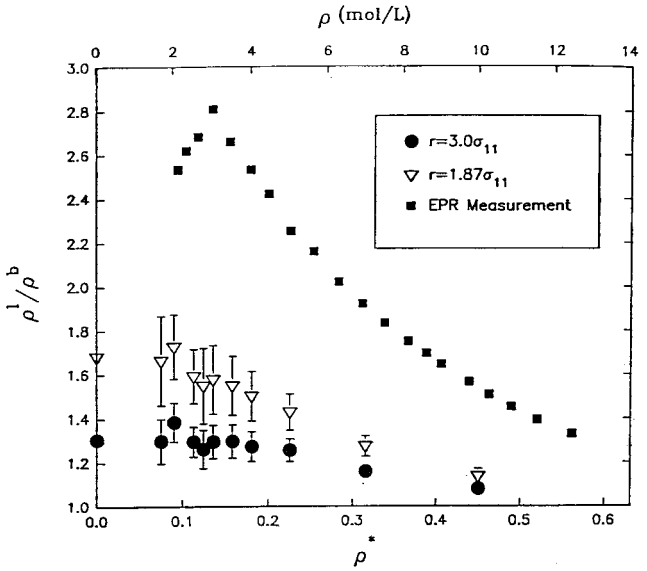

Figure 18. Relative local densities $\tilde{\rho}_l$ vs bulk density for DTBN in ethane at $T_r = 1.08$, extracted from EPR measurements and from molecular dynamics simulation of a Lennard-Jones model for this system, using two different radial cutoffs (eqs 3 and 4). ρ^* is in Lennard-Jones units. (Reprinted from ref 62 with permission of the American Institute of Chemical Engineers. Copyright 1993. All rights reserved.)

ibility.[129] However, at present there is not enough data to back up such speculation. Returning to the main argument, we note that the location of the maximum in $N^{ex}(\rho_r)$ computed by Flanagin et al.[80] appears to be relatively insensitive to temperature changes. At $T_r = 1.0$ the maximum appears to fall at $\rho_r \approx 0.5-0.6$, but the absence of data between $\rho_r \approx 0.5$ and $\rho_r = 1$ makes this conclusion shaky. At $T_r = 1.1$ the maximum falls between $0.3 < \rho_r < 0.5$, yet at $T_r = 1.3$, the maximum appears to shift back toward higher densities, $\rho_r \approx 0.5$. Hence, no clear trend with temperature is discerned from these results.

The local density enhancements $\tilde{\rho}_l$ vs ρ_r computed from a few of the Lennard-Jones simulations have been used to provide a comparison for local density enhancements extracted from experiment. Knutson et al.,[46] who used Lennard-Jones parameters appropriate for pyrene in CO_2, compared their simulated relative local densities with those extracted from pyrene emission intensities in SC CO_2, Figure 12 (see section III.A.1.b). By choosing a cutoff radius of $R = 1.94\sigma$, these authors obtained nearly quantitative agreement between $\tilde{\rho}_l(\rho_r)$ computed from simulation and experiment. However, it must be noted that the experimental data extends only down to $\rho_r = 0.5$, whereas the maximum in $\tilde{\rho}_l$ observed from simulation occurs at $\rho_r \approx 0.3$. In contrast, Randolph, O'Brien and co-workers[62,89,182] compared local density enhancements extracted from spectral shifts of the EPR hyperfine splitting constant for DTBN[62] in SC CO_2, ethane (Figure 18), and CHF_3, with those computed from simulations using appropriate Lennard-Jones parameters. In all cases, the EPR results substantially exceeded the simulated values of $\tilde{\rho}_l$ for the same reduced temperature isotherm, with maximum EPR values attaining 200% to 500% enhancements and the simulated values attaining enhancements of only 20% to 50%. While most of the simulations used a cutoff radius including approximately two solvent shells,[89] use of a smaller radius incorporating just the first shell only brought the simulation value up to a 70% enhancement, Figure 18.[62] Additionally, the experimental $\tilde{\rho}_l(\rho_r)$ curves exhibit sharp maxima falling in the range $0.35 < \rho_r < 0.6$, while the simulation curves are all relatively flat at low reduced densities, with no discernible peak. Such consistent overprediction of local density enhancements by experiment as compared to simulation results has also been reported by Maroncelli[75] for fluorescence spectral shifts of various probes in a series of SC solvents. At present, the origins of these disagreements are unknown.

2. REPULSIVE AND WEAKLY ATTRACTIVE SOLUTES. Finally, Tom and Debenedetti[61] examined $\tilde{\rho}_l(\rho_r)$ for a repulsive Lennard-Jones system, Ne in SC Xe. As is also apparent in Chialvo and Cummings' [47] evaluation of the nondivergent component of the partial molar volume (see section III.A.2.a) for repulsive systems, the behavior of $\tilde{\rho}_l(\rho_r)$ for the repulsive system, Ne in SC Xe, is qualitatively different than that observed for the attractive solute−solvent systems discussed above. For any cutoff radii at or beyond 1.4σ, which is the position of the first minimum in the high density $g_{12}(r)$, the relative local density is minimized at $\rho_r \approx \rho_c$, rather than at values of $^1/_2$ to $^1/_3$ ρ_c, as are generally observed for the extrema in relative local density enhancements for attractive systems. And, for a cutoff of $R = 1.5\sigma$, only an 8% depletion is observed; the degree of depletion diminishes with increasing cutoff radius, as would be expected. Similarly, Munoz and Chimowitz's[126] study of what appears to be a weakly attractive system shows virtually no enhancement (or depletion) for densities $\rho_r > 1$ (using $R = 3.0\sigma$). There is a transition in behavior around the critical density, to yield about a 3% enhancement at densities $\rho_r < 1$.

v. Spectral Shifts and Solvation Free Energies. Despite the number of experimental studies focused on spectroscopic shifts in SCFs, only one recent theoretical study evaluates spectroscopic shifts. Adams[130] performed molecular dynamics simulations of benzene in Lennard-Jones Ar in order to obtain equilibrium configurations of the solvent for use in computing spectral shifts. He then considered both short-range repulsions and the collective polarization modes of SC Ar when evaluating spectral shifts for the electronic excitation of benzene. The bulk density dependence of the spectral shifts was found to correlate with that of the first shell coordination number, as expected. Additionally, Adams considered the strength of the Ar−benzene polarization coupling as a function of the distance from the solute and found that 90% of this polarization coupling arises from Ar atoms residing in the first solvation shell. Since the repulsive contributions are by nature first shell effects, it follows that electronic spectral shifts in such nonpolar systems indeed probe only the very local solvent environment, i.e. the first solvation shell.

A quantity often related to spectral shifts is the variation in the solute's solvation free energy upon

excitation. Solvation free energies and related quantities have been examined in Lennard-Jones systems by integral equation techniques.[47,61,126] Chialvo and Cummings[47] and Munoz and Chimowitz[126] showed that the solute chemical potential is nondivergent as the critical point is approached and that it can be written in terms of direct correlation function integrals.[47] Hence, the range over which the solvent environment, and thus solvent density enhancements, can affect solute energetics is given approximately by the range of the solute−solvent interaction potential. This result can also be seen from the Kirkwood coupling equation, which gives the chemical potential as a radial integral over the interaction potential times a modified radial distribution function (see, e.g. eq 1 of ref 126). Indeed, Munoz and Chimowitz[126] showed for naphthalene in SC CO_2 that the chemical potential attained 90% of its total value within a range of less than 3.5σ, and that this result is relatively insensitive to state point. Tom and Debenedetti[61] observed a similar range dependence for the fugacity coefficient in the same system. However, these authors observed (at $T_r = 1.07$) that if 99% of the final value is required instead, the range necessary to achieve this is nearly 5σ at a bulk density of $0.85\rho_c$, compared to 3.5σ at $0.3\rho_c$ and $1.3\rho_c$.

Although the range over which density enhancements affect solvation free energies in dipolar solute−solvent systems has not been studied by simulation, this range dependence has been studied with a compressible continuum model, which include only direct density enhancement effects (see section III.A.2.c), for ions and polar molecules in SC water.[129] Luo and Tucker[129] found that although an ion in SC water at a highly compressible state point (e.g. $T_r = 1.01$, $\rho_r = 0.77$) can induce direct density enhancements out to distances of more than 25 Å, which include over 120 excess water molecules, only the enhancements within roughly the first two solvation shells, e.g. out to 6 Å, which includes an excess of only 15 water molecules, contribute substantially to the solvation energy. It particular, it was found that by 6 Å the solvation energy stabilization due to the density enhancements attains 83% of its total value, whereas the excess number of solvent molecules attains less than 12% of its total number by this point.

c. Continuum Models. *i. Distribution Functions.* Electrostatic continuum solvation models, in which the solute is treated as a charge distribution in a cavity which is itself embedded in a continuous dielectric medium characterized by the solvent's dielectric constant ϵ_s, provide a computationally efficient alternative to computer simulations.[131−133] In the traditional implementation of such continuum models, the dielectric constant everywhere outside of the molecular cavity is taken to be fixed at the bulk value ϵ_s. However, because the dielectric constant reflects the dipole density (and/or the net polarizability per unit volume), the use of a uniform dielectric constant implies the assumption of a uniform solvent density throughout. As has been pointed out by a number of authors,[134−139] this assumption is clearly poor for highly compressible SCFs in which the local solvent density is expected to respond to the presence of the solute. In particular, the interaction between the solute-induced electric field and the surrounding solvent dipoles will cause a compression of the surrounding solvent, i.e. electrostriction, or in the terminology of the SCF literature, a density enhancement.

To allow for the presence of such electrostriction effects, so-called compressible continuum models have been developed.[135,137,140] The first model, developed by Wood, Quint, and Grolier,[135,141] adds electrostriction effects into the Born solvation model[142] and is thus restricted to spherical ions. Luo and Tucker[137,140] generalized the method of Wood et al. to the case of molecular solutes by using a numerical grid based algorithm[143] for solving the electrostatic equations in the presence of electrostriction. In both methods, self-consistent solution of the electrostatic equations in the presence of a compressible dielectric medium yields the equilibrium solvent density distribution around the solute, $\rho_l(\mathbf{r})$. When radially averaged, this distribution becomes comparable to radial distribution functions computed from computer simulation, except that the continuum model distribution $\rho_l(r)$ contains no molecular structure effects. An important aside is that compressible continuum models allow the solvent density to respond to the solute-induced potential at each point in space **r**, but not to the solvent density at other points in space (except insofar as such fluctuations alter the electrostatic potential at **r**), and thus include only direct density enhancement effects (section II.A).

A less sophisticated model which accounts for electrostriction in the first solvation shell is the concentric shell model,[76] in which a Langmuir adsorption analogy is used to predict the first shell coordination number around specific atomic ions at each state point. The ion is then embedded in an incompressible dielectric continuum which is described by the dielectric constant corresponding to the first shell coordination number in a shell around the ion and by the bulk solvent dielectric constant at longer distances. Finally, although there is no fundamental restriction of these continuum methods to SC water solution, this is the only application to which they have so far been applied.

Comparison of density distributions predicted by compressible continuum models with those computed from molecular dynamics simulations have proven the veracity of these continuum model predictions, within the structureless approximation of these models.[128,144] In particular, compressible continuum models suggest that the direct density enhancements[10,137] around ions in SC water extend out to very long distances from the solute when the solvent compressibility is large,[129,135−137,144,145] and these long-range tails of the distribution are in good agreement with those observed in molecular dynamics simulation.[144,146] For example, Flarsheim et al.[145] found at $T_r \approx 1.02$ and 25 MPa that the density 10 Å away from I^-, a 2.2 Å radius ion, is ~0.4 g cm^{-3}, which is still ~30% greater than the bulk density of ~0.3 g cm^{-3}. The observation of significant density enhancement effects out to 10−15 Å is common,[128,129,136,144,145]

and even in near-critical subcritical water ($T_r = 0.92$, $\rho_r = 2$) a density enhancement of ~18% is observed 10 Å from a 2 Å radius ion.[135] The reason for such long-range enhancements has been outlined nicely by Luo and Tucker,[129,137] who show that the compression of a solvent in response to an electric field is a highly nonlinear function when the solvent has a large bulk compressibility. As a result, the small residual fields far from the solute may induce significant compression. Note that Luo and Tucker[144] also analyzed the compression observed at state points having the same bulk compressibility but different bulk densities. They found that, given the same bulk compressibility, a greater absolute density enhancement will be observed under the lower density conditions, consistent with other observations that local density enhancements are maximized at densities below the critical density. Note that Wood et al.[128] have considered the effect of dielectric saturation on the formation of local density enhancements.

As a result of the long range of the direct density enhancements, the total excess number of water molecules associated with these enhancements, N^{ex}, can be very large, because the $4\pi r^2$ factor means that small excess densities at long range correspond to many excess molecules. For example, Quint and Wood[136] found an effective excess of 434 water molecules around an ion at $T_r \approx 1.0$ and $P = 22.15$ MPa, while Luo and Tucker[129] observed an excess of more than 120 molecules at $T_r = 1.10$ and $\rho_r = 0.77$. These authors[144] found that around a negative ion, the compressible continuum model estimate of N^{ex} underestimates the value predicted from simulation because of the neglected specific interactions (e.g. hydrogen bonding) which enhance the first shell density. Finally, it is worth noting that because of the very strong fields around ions, density enhancements in the first solvation shell are observed over very broad ranges of thermodynamic condition, both in continuum[145,136] and in molecular dynamics calculations.[80,81]

ii. Solvation Free Energies. Continuum models can also be used to evaluate free energies of solvation, and a number of insights have been gained by applying continuum solvation models to interpret solvation and reaction in SC water. First, application of standard, incompressible continuum models can provide a reasonable description of solvation over a wide range of conditions in SC water. However, as shown by Rossky, Johnston, and co-workers,[76,139] incompressible models work well only when the solute cavity radii is optimized for SC conditions. This reoptimization is not needed when a solvation model incorporating electrostriction effects, such as Wood et al.'s[135] model or the concentric shell model,[76,139] are used, thus demonstrating that this reparametrization is really providing a correction for the neglected electrostriction.[76] The reason that one can correct for electrostriction within the framework of an incompressible continuum model is probably because the first shell enhancement around atomic ions in SC water is relatively insensitive to thermodynamic condition over a fairly broad range of conditions. For example, molecular dynamics simulation predicts[76] the coordination number around Cl^- in (SPC/E) water at $\rho = 0.087$ g cm^{-3} and $T_r = 1.05$ to be the same as in water at $\rho = 1.0$ g cm^{-3} and $T = 298$ K. Similar invariance is observed across SC conditions with densities ranging from $\rho_r = 0.087$ to $\rho_r = 0.5$ and temperatures up to 40% over T_c.

However, very near to the critical point where the compressibility is large, local density enhancements extend beyond the first solvation shell and become sensitive to thermodynamic condition. As a result, incompressible continuum models fail to accurately predict solvation energies,[134,137−139,144,147] and even models including first shell enhancements (but no longer-range enhancements) may fail.[76] For example, Luo and Tucker[137] showed using their compressible continuum model that at $T_r = 1.01$ and $\rho_r = 0.8$, a state point which has a compressibility 15 times that of an ideal gas under the same conditions, solvent compression effects stabilize the phenoxy anion (PhO^-) by 14.4 kcal/mol, whereas at $T_r = 1.01$ and $\rho_r = 2.0$, where the compressibility is only 0.23 times that of an ideal gas, solvent compression stabilizes the phenoxy anion by only 4.5 kcal/mol, an effect attributable to first shell enhancements.

Most of the continuum model work on SC water has been directed toward understanding solvent effects on reaction energetics. Thus, the focus has been on the computation of the difference between the solvation energies of the reactant and the activated complex, $\Delta F^{\ddagger}_{solv}$. Bennett et al.[138] examined the $Cl^- + ClCH_3$ S_N2 reaction in SC water at three state points. These authors compared incompressible continuum model calculations of $\Delta F^{\ddagger}_{solv}$ with those computed from molecular dynamics simulation.[80,148] They found that readjustment of the cavity parameters led to agreement between the continuum and simulation results at two of the state points, but significant disagreements remained at the state point $T_r = 1.0$ and $\rho_r = 0.5$. Luo and Tucker[144] then studied this same reaction using their compressible continuum model and found that without readjusting the cavity radii they could reproduce the molecular dynamics values for the relative solvation energies, $\Delta F^{\ddagger}_{solv}$, to within 1 kcal/mol at all 3 state points considered by Bennett et al.[138] and to within 1.7 kcal/mol under ambient conditions. At $T_r = 1.0$ and $\rho_r = 0.5$, where the greatest local density enhancements were predicted by the compressible continuum model[137] (and observed in simulation[80]) $\Delta F^{\ddagger}_{solv}$ was found to be increased by 7 kcal/mol as a result of the electrostriction, which is greater around the reactants than around the activated complex, and stabilizes the reactants relative to the activated complex.[144]

Tomasi and co-workers[147] studied this reaction with a continuum model in which position-dependent dielectric constants predetermined from molecular dynamics simulation were incorporated. Not surprisingly, these authors obtained nearly the same results as did Luo and Tucker,[144] thus confirming both the predictive capabilities of these latter authors' compressible continuum model and the necessity of including density inhomogeneities explicitly when considering compressible state points.

Tucker and co-workers' [134,137,140] study of the anisole hydrolysis reaction in SC water further confirm these conclusions. Here, the state-point dependence of the density inhomogeneity effects is highlighted. In particular, when electrostriction is neglected, the change in $\Delta F^{\ddagger}_{solv}$ when going from $\rho_r = 0.8$ to $\rho_r = 1.6$ along the $T_r = 1.01$ isotherm is -16.1 kcal/mol. When electrostriction is included, this prediction drops to -4.1 kcal/mol,[137,140] in much better agreement with the value of -1.5 kcal/mol extracted from experiment.[149]

B. Dynamic Measurements

1. Rotational Lifetimes

a. Fluorescence Anisotropy. Anisotropic fluorescence emission provides a means for evaluating the rotational lifetimes of solute probe molecules. Not surprisingly, solute rotation times in liquids are strongly influenced by solvent viscosity, and hence, solute rotation times should provide a sensitive probe of local solvent environments in SCFs. However, a series[98,99,150,151,182] of attempts to use solute rotational times to probe SCF environments has resulted in disagreement, both about the interpretation of the measured lifetimes and about the lifetimes themselves.[99]

In 1992, Bright and co-workers[98] observed the suprising result that along a near-critical isotherm of SC N_2O ($T_r = 1.01$), the rotational lifetime of PRODAN[98] decreases dramatically with *increasing* solvent viscosity as the bulk density is increased beyond the critical density. A subsequent study from this group[151] observed the same behavior for the rotational lifetime of BTBP[151] in SC CO_2, CHF_3, and ethane. In contrast, Heitz and Maroncelli[99] (who used a time-domain spectroscopy rather than the frequency-domain method of Bright's group) observed qualitatively "normal" behavior for BTBP in SC CO_2, i.e. they observed the rotational lifetime to increase with increasing viscosity. While the verdict is still out, there are a few reasons to believe the more recent data.[99] First, the local densities required to explain Bright's data are abnormally large, e.g. a factor of 4 enhancement. And, perhaps more disconcertingly, the relative local density enhancement is found to peak at densities very near to the critical density, whereas a phenomena probing the very local solvent environment would be expected to yield a local-density-enhancement maximum at much lower densities. The alternative argument that the increasing rotational lifetimes is a reflection of the weak divergence of the viscosity at the critical point (critical slowing down) is unlikely as well, because the substantial increases in the lifetimes were also observed at densities well removed from the critical density, with substantial enhancements of factors of 2−4 being observed at $\rho_r \approx 1.5$.[151] Additionally, the "normal" behavior observed by Heitz and Maroncelli for TPP[99] and PEA,[99] as well as for BTBP, was also observed by Anderton and Kauffman[150] for DPB[150] and HMS[150] in SC CO_2.

While Anderton and Kauffman[150] and Heitz and Maroncelli[99] both observed "normal" behavior, the methods these groups used for extracting local density enhancements from the rotational lifetimes differ and, in fact, lead to qualitatively different conclusions.[99] In particular, Anderton and Kauffman's[150] interpretation of their data leads them to conclude that local density enhancements occur around HMS but not around DPB. In contrast, Heitz and Maroncelli's[99] analysis of Anderton and Kauffman's data leads these authors to conclude just the opposite, that there are density enhancements around DPB but not around HMS. While both groups' methods rely on the modified Stokes−Einstein−Debye model with stick boundary conditions to predict the expected rotational lifetimes in the absence of solvent density inhomogeneities, they predict different density dependencies for the boundary-condition factor. In particular, the Stokes−Einstein−Debye model gives the rotational time as

$$\tau_R = \frac{\eta V_p}{kT} fC \tag{5}$$

where V_p is the solute volume, f is a calculable shape factor for stick boundary conditions on nonspherical molecules, η is the viscosity, C is a boundary condition parameter, and k is Boltzmann's constant. Heitz and Maroncelli provide evidence that C should be relatively invariant to changes in density, while Anderton and Kauffman assume a theoretically justified density dependence for this quantity. Additionally, Anderton and Kauffman add a zero-viscosity, free-rotor lifetime as an offset to the Stokes−Einstein−Debye model. One disconcerting feature of the Anderton−Kauffman model, however, is that in its usual application, it is assumed that the relative local density enhancement, $\tilde{\rho}_l$, remains constant as the bulk density varies. And, this assumption appears to be supported[150,152] by the data, at least within limits of the scatter, in spite of the fact that simulation and spectroscopic shifts clearly show this to be a poor assumption in general. The question of which method will provide the best method of analysis of rotational data is still a matter of debate, and the uncertainty in such analyses makes it difficult to extract meaningful density enhancements from such experiments.

An important note is that the density enhancements extracted by Heitz and Maroncelli[99] for PEA were found to be identical, within error, to those they extracted from fluorescence emission frequency shifts in the same system. And, while this does suggest some validity to these authors' analysis of the rotational lifetimes, there is, in fact, no requirement that these enhancements need agree with one another, as the two measurements provide physically different probes of the local solvent environments and may probe on different length scales.[99] As a cautionary note along these lines, Heitz and Maroncelli also examined the radiative lifetimes for PEA and found that this quantity shows no evidence of local density enhancements.

b. NMR. NMR measurement of spin−lattice relaxation times can be used to obtain solute rotational correlation times τ_R, which, as discussed in the previous section, provide a sensitive probe of the local

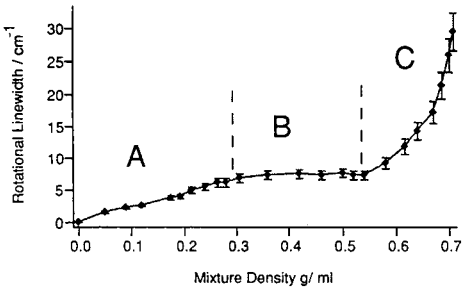

Figure 19. Rotational Raman line width of H_2 ($S_0(1)$) against bulk density in a single-phase mixture of CO_2 with 18% H_2 at 297 K; T_c = 304.1 K for CO_2 and 33.2 K for H_2. (Reprinted from ref 154, copyright 1993, with permission from Elsevier Science Publishers.)

solvent viscosity. These measurements may also provide the spin angular momentum correlation time τ_J, which also provides information about the local solvent environment, as it depends linearly on the time between molecular collisions. Grant and co-workers[152] used such NMR measurements to extract rotational correlation times for methanol and 1-decanol in subcritical and SC CO_2 as a function of density from $0.9 \lesssim \rho_r \lesssim 2$ for temperatures $0.95 \leq T_r \leq 1.14$. These authors used the method of Anderton and Kauffman[150] (see previous section) to extract local density information from the measured rotational times. Unfortunately, these authors combined their data for all temperatures when performing this analysis. Nevertheless, they obtained a reasonable fit to the Anderton−Kauffman model with an assumed local density enhancement of 15% around 1-decanol and 35% around methanol. Recall that only one enhancement value is obtained because this model assumes the relative density enhancement to be independent of the bulk density. Interestingly, these authors[152] also measured the spin angular momentum correlation times for methanol, and, using a method analogous to the Anderton−Kauffman method for τ_R to extract a constant local density enhancement value from the measured τ_J's, they obtained a value of 30%, in good agreement with the τ_R results. Evilia and co-workers[153] examined the angular momentum (τ_J) and rotational (τ_R) correlation times for naphthalene in subcritical and SC CO_2. They observed τ_R to remain virtually invariant despite large, simultaneous changes in both density and temperature, whereas they found τ_J to take on surprisingly small values quite suddenly under just-subcritical liquid conditions. Although these authors attribute this abnormal behavior to solvent density enhancements, the unexplained disparate behavior of τ_J and τ_R suggests that something else may be going on.

c. Raman Line Widths. Howdle and Bagratashvili[154] examined the rotational Raman line width of H_2 (S_0 (1)) in SC CO_2 (18 mol % H_2) at T = 297 K, which is in the mixture's supercritical regime, as a function of density. These authors observed (Figure 19) the classic three-regime signature of local density enhancements (section II.C and III.A.1). That is, the line widths were observed to increase slowly at low densities, remain nearly constant at intermediate densities, and rise rapidly at high densities. Since

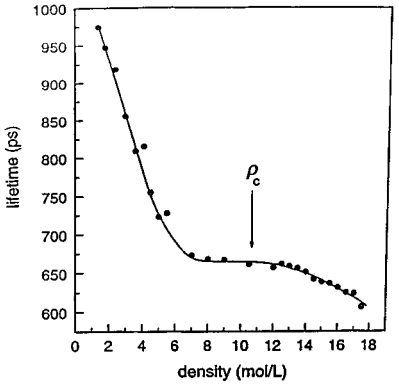

Figure 20. Vibrational lifetime for the T_{1u} asymmetric stretching mode of $W(CO)_6$ in CO_2 vs density at 33 °C ($T_r \approx 1.01$). Infrared absorption peak positions for this same mode under these conditions appear in Figure 9. (Reprinted with permission from ref 100. Copyright 1997 American Insitute of Physics.)

the rotational line width is a probe of the first solvation shell, the region of invariance suggests a region in which local density enhancements have yielded a nearly complete first solvation shell, and no further changes are observed until high-density compression of this solvent shell sets in. However, no adequate theory was available for the quantification of these likely enhancements. Another interesting observation made by the authors is that the line shapes cease to be Lorentzian at the high densities, a feature they attributed to an inhomogeneous distribution of local environments and, hence, of dephasing rates.

2. Vibrational Energy Relaxation

The rate at which the excess energy of a vibrationally hot solute is dissipated to the surrounding solvent is a sensitive probe of solvent properties and has been shown to be sensitive to solvent density, both in gases and in liquids.[155−158] Recently, Troe and co-workers,[94,159,160] Fayer and co-workers[79,100,101] and others[161] performed experimental investigations of vibrational energy relaxation rates in SCF solvents (CO_2, ethane, propane, and CHF_3) along near-critical isotherms. Fayer's group considered relaxation from the first excited vibrational state of the T_{1u} asymmetric CO stretch mode in $W(CO)_6$,[79,100,101] whereas Troe and co-workers considered relaxation of highly vibrationally excited (e.g. ∼18 000 cm^{-1}) azulene[94,159] and 1,3,5-cycloheptatriene.[160] Despite the very different vibrational processes considered by these groups, the classic three-regime behavior was observed in all cases in which a sufficient range of pressures (densities) were considered, e.g. see Figure 20. Additionally, in three of these studies,[94,100,101] spectroscopic shifts were also evaluated, and the bulk density dependence of these shifts were found to mirror the behavior of the lifetimes, e.g. Figure 9. Such results are suggestive of local density enhancement effects, and the signature of these effects in the vibrational energy relaxation data imply that such relaxation dynamics are affected primarily by the nearby solvent molecules, at least in the systems considered.

That vibrational relaxation should probe only the very local environment is, in fact, generally expected; however, Cherayil and Fayer[102] have questioned the local density enhancement interpretation of the vibrational lifetime data. These authors developed a theory of vibrational lifetime which, near the critical point, they evaluate in the long wavelength hydrodynamic limit. On the basis of the ability of this long wavelength theory to correctly predict the qualitative behavior of the measured lifetimes, these authors suggested that the long range critical fluctuations play a crucial role in determining the vibrational lifetimes.[100,102] In apparent contrast, Troe and co-workers[94] were able to fit their measured lifetime data by incorporating local density enhancements computed from simulated radial distribution functions of an attractive hard-sphere solute in a Lennard-Jones solvent into isolated binary collision theory. Note, however, that these authors' fits contained two adjustable parameters and were only performed on the $T_r \approx 1.3$ isotherm due to simulation difficulties encountered on more near-critical isotherms.

Recent work by Goodyear and Tucker[68] show that these two views on vibrational relaxation—that which says the near-critical behavior of the relaxation times arises from long-range critical fluctuations and that which says they arise from local density enhancements—are not necessarily incommensurate. These authors computed vibrational relaxation rates from a Lennard-Jones diatomic in a two-dimensional Lennard-Jones SCF along a near-critical isotherm. Because the interaction of each solute atom with the solvent atoms was taken to be the same as the interaction of the solvent atoms with each other, the system closely resembles a neat fluid; yet it was found to exhibit the same invariance of the lifetime to bulk density changes at densities below and around ρ_c as was observed in the experiments. The authors showed that this self-similar solute/solvent system supported *average* local density enhancements around the solute and that the magnitude of these enhancements as a function of bulk density correlates with the observed deviation of the computed lifetimes from those predicted on the basis of high-temperature simulations. Hence, these authors attribute the observed lifetime behavior to average local density enhancements. However, they argue that at least in this self-similar system, the local density enhancements can be viewed as a direct consequence of the long-range critical fluctuations (see section IV.B.1 and Figure 1), thus providing a plausible connection between the local density and critical fluctuation viewpoints.

C. Negative Results

While in a number of studies density inhomogeneity effects were not observed, in most of these studies (see e.g., refs 86, 99, and 162−164), the apparent absence of these effects can be attributed to one of two things. First, and most common, is the consideration of SC conditions under which local density effects are likely to be small. For example, consideration of an isotherm which is insufficiently close to T_c (and how close is close can be sensitive to the nature of the system), or of an insufficient range of densities (or number of density points), will minimize (or obscure) local density inhomogeneity effects. In particular, studies in which only densities greater that ρ_c are considered tend not to show local density inhomogeneity effects. Second, observation of local density inhomogeneity effects is conditional upon choice of a probe which is sensitive to these effects (see for example the discussion of ref 99 in section III.B.1.a). Additionally, the effect of local density inhomogeneities on some solute properties, such as diffusion rates[62,71,165−169] and interaction-induced Raman light scattering[170] have have only begun to be carefully investigated, and, hence, it is as yet unclear whether experimental observations using these probes can be interpreted in terms of local density inhomogeneity effects.

Additionally, there are three studies, all conducted in neat SCFs, in which expected local density enhancement effects do not appear to be observed. Raman spectroscopy studies of the vibrational frequency of the CH stretch in SC ethane were performed by Ben-Amotz et al.[171] at reduced temperatures of $T_r = 1.02$ and $T_r = 1.15$ over a broad range of densities, from $\rho_r \approx 0.1$ to $\rho_r \approx 2.3$. These authors found the frequency shift data taken at both temperatures to be nearly coincidental, and that the density dependence of the shifts could be well fit using a hard-sphere model. These behaviors both point to an absence of local density enhancement effects.

Although computer simulation has shown that average local density enhancements should be expected in a pure SCF when critical fluctuations are present,[10,68] it is not known how close one needs to be to the critical point to observe these effects. That is, the region of the phase diagram in which local density enhancements are present in attractive solute−solvent systems, which we know something about, is likely to be broader than the range over which such effects are important in neat SCFs. Thus, Ben-Amotz's data[171] suggest that a temperature of $T_r = 1.02$ is insufficiently close to the critical isotherm for the average local density enhancement to significantly exceed the bulk density. Note, however, that the data point at $T_r = 1.02$ and $\rho = \rho_c$ falls slightly below the fit. While this deviation is small, and possibly not significant, it suggests that perhaps at a lower temperature the local density enhancements predicted by computer simulation might be found.

Okazaki and co-workers[172] used both Raman scattering techniques and molecular dynamics simulation to examine rotational relaxation times in neat CHF_3, also along the $T_r = 1.02$ isotherm. While these authors did observe a minimum in the relaxation times near the critical density, this behavior (being a minimum, rather than an invariance in an otherwise monotonically increasing function) is not easily interpretable in terms of local density enhancement effects. Of more interest are the molecular dynamics snapshots at $T_r = 1.02$ and $\rho \lesssim \rho_c$, which show some evidence of fairly short-ranged critical fluctuations. Further analysis would be desirable, to determine the

degree to which such fluctuations are present (and whether they were restricted by the small size of the simulation system) and what local density enhancements should be expected under these conditions. In comparison with Ben-Amotz's results,[171] the question also arises as to what effect the nature of the potential interactions have on the proximity to the critical point at which local density enhancements effects will be observed in neat SCFs.

In contrast, Saito and co-workers[173] found the IR absorbance intensity of the Fermi resonance in neat SC CO_2 at temperatures below $T_r \approx 1.05$ to show substantial deviations from the high temperature behavior. In fact, these authors observe the intensity to become relatively invariant to bulk density changes near the critical density on these near-critical isotherms. However, if local density enhancements were present, the intensity would be expected to *exceed* that observed at higher temperatures, but they were instead found to be *smaller* than the higher temperature results. These results still await explanation.

IV. Additional Characteristics of Local Density Inhomogeneities

A. Asymmetries in the Local Density

Both theoretical and experimental investigations have been directed toward elucidating the spatial distribution of local densities around molecular solutes.[108,137,144,152,167,174,175] In particular, functional groups having strong potential interactions with the solvent may act more "attractively" than other molecular sites, thus inducing greater density enhancements around the functional end of the molecule. This behavior was demonstrated by Luo and Tucker,[137,144] who used their compressible continuum model (see section III.A.2.c.i) to predict the spatial distribution of local solvent densities around reactive solutes in SC water, which they presented as contour plots. For the ion−dipole complex $Cl^-\cdot CH_3Cl$ at $T_r = 1.3$, $\rho_r = 0.5$ ($\rho = 0.16$ g cm^{-3}), the local density near the charged chlorine was ~0.4 g cm^{-3}, approximately 50% higher than was found near the neutral chlorine, see Figure 21.[144] Similar results[137] were obtained for an intermediate along the anisole hydrolysis reaction path, $PhO(\delta^-)\cdots CH_3\cdots OH_2(\delta^+)$. For this complex, the local density near the partially charged $-OCH_3OH_2$ group was found to be nearly 200% greater than around the phenyl group at $T_r = 1.08$ and $\rho_r = 0.8$, but only about 50% greater than around the phenyl group when the bulk density is increased to $\rho_r = 1.6$. Additionally, these authors found that the local density near the very negative oxygen atom in the PhO^- anion is substantially greater than near the phenyl group, but that at further distances from the molecule the density contours became roughly spherical (centered around the oxygen), reflecting the long-range view of PhO^- as a spherical ion.

Inomata, Saito, and Debenedetti[167] found similar behavior when comparing the first-shell solvent enhancements out-of and in-the-plane-of a benzene molecule in SC CO_2 at $T_r = 1.05$. Using molecular dynamics simulations, these authors found the ratio of the out-of to in-the-plane radial distribution function first peak heights to be 3.5 at $\rho_r = 0.5$ where density enhancements out-of-plane are large, but only 2 at $\rho_r = 2$, where the overall density enhancements are reduced. Iwai and co-workers[174] examined solute-site-specific radial distribution functions for straight chain alcohols and alkanes in SC CO_2 at $T_r \approx 1.01$ and $P_r \approx 1.37$ by Monte Carlo simulation. They found, for example, that in cetyl alcohol the first-peak enhancement around the OH group and α-carbon were nearly 50% greater than those around carbons further down the carbon chain.

Similar observations have also been made on the basis of experimental data. In particular, Wada and co-workers[108] used FT-IR intensities to extract local densities around various functional groups (associated with particular vibrational modes) on substi-

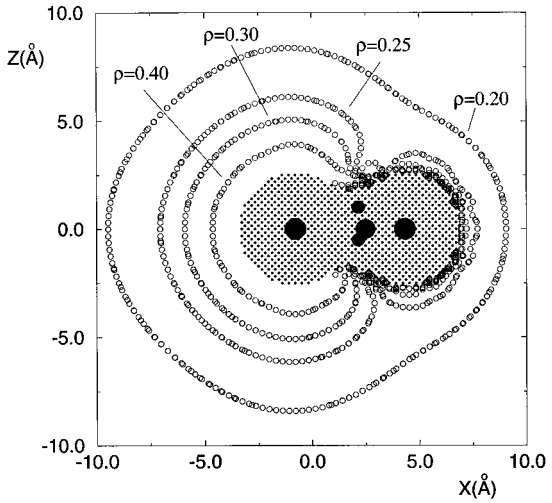

Figure 21. Solvent density contours, computed from a compressible continuum solvation model, around the ion−dipole complex on the $Cl^- + CH_3Cl \rightarrow ClCH_3 + Cl^-$ reaction path in water at $T_r = 1.3$ and $\rho_r = 0.50$. Density contours are labeled in g cm^{-3} and the bulk density is 0.162 g cm^{-3}. (Reprinted from ref 144. Copyright 1997 American Chemical Society.)

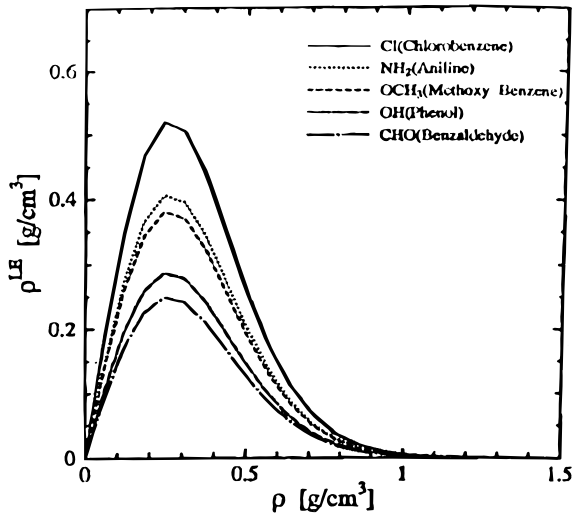

Figure 22. Density dependence of the local excess density $\rho_l^{ex} = \rho_l - \rho$ about subsituted group consituents in various substituted benzene compounds in CO_2 at 318.2 K ($T_r = 1.05$). Local densities were extracted from IR molar absorption coefficients, see Figure 13. (Reprinted from ref 108. Copyright 1997 American Chemical Society.)

tuted benzene compounds in SC CO_2 at $T_r = 1.05$. The bulk density dependence of the functional-group-specific local densities was observed to be the same for all functional groups, Figure 22, exhibiting a maximum at $\rho_r \approx 0.55$. The maximum local density around the functional groups was found to range from 1.4 (methoxy benzene) to 2.1 (chlorobenzene) times that found around the C−C constituents.

Grant and co-workers'[152] analysis of rotational correlation times of 1-decanol in SC CO_2 yielded evidence of site-specific enhancements around the functional end of this solute; however, the difficulties inherent in the interpretation of these data discussed in section III.B.1 unfortunately makes their results inconclusive. Site-specific local density enhancements were also proposed by Anderton and Kauffman[150] to explain their rotational data, but this again must be considered inconclusive.

B. Distributions of Local Environments

1. Simulation

Until now, we have focused on the average local densities found around solutes (or tagged solvent molecules) in SCFs. However, a number of investigators[10,62,66,113,121,168,176,183] have used computer simulation to determine the distribution of local environments, i.e. of local densities, experienced by the solute in the equilibrium ensemble. Not surprisingly, as the critical point is approached and critical fluctuations begin to grow in, the distribution of local densities broadens dramatically.[10,168] In particular, Luo et al.[168] determined the local densities within individual blocks on a grid[82] for a pure two-dimensional Lennard-Jones SCF at a bulk density $\rho_r = 1.0$ ($\rho = 0.34$ Lennard-Jones units). They found that as the temperature decreased from $T_r = 1.52$ to $T_r = 1.09$, the standard deviation in the observed block densities nearly doubled, from 0.9 to 0.18 Lennard-Jones units (although these results are very sensitive to block size[82]). Note that for such a non-atom-centered measure of the local densities, the *average* block density must remain equal to the bulk density. Tucker and Maddox[10] considered the distribution of local densities around a tagged solvent atom in the same system[177] at a bulk density $\rho_r \approx 0.86$ (0.30 Lennard-Jones units). The local density around a tagged solvent particle at any time t, $\rho_l(t)$, was determined by the number of other solvent atoms within a radius $R = 3.1\sigma$ of the tagged particle. As the temperature is decreased from $T_r = 10.6$ to $T_r \approx 1.17$, the full width at half-maximum of the distribution of local densities, $P(\rho_l)$, was found to increase by a factor of 2, from 0.18 to 0.36, Figure 16. (Note again that the exact value obtained will be sensitive to the size of the local region considered.) Additionally, as the bulk density is tuned to lower or higher densities, the distribution of local densities was found to narrow substantially,[64] as would be expected upon moving away from the critical region. In an earlier work, Martinez, Ravi, and Tucker[121] classified atoms in this two-dimensional Lennard-Jones system as being in low, average or high local density regions based on their instantaneous local densities. These authors found that the number of high-, average-, and low-density atoms remained roughly constant over time, constituting, at $T_r \approx 1.6$ and $\rho_r \approx 0.86$ for a cutoff $R = 3.1\sigma$, approximately 50%, 35%, and 20% of the total number of atoms, respectively. This propensity for the majority of the atoms to be found in high-density regions (cf. Figure 1) increases as the critical point is approached and the correlation length increases,[64] and it causes the maximum in the atom-centered local density distribution $P(\rho_l)$ to shift to densities greater than the bulk value.[10,68] It is this shift which causes the average (atom-centered) local density $\langle\rho_l\rangle$ to exceed the bulk density in neat, near-critical SCFs, providing a connection between the observed local density enhancements and the critical fluctuations.

This perspective can also be applied to interpret local density enhancements around attractive and repulsive solutes. Tucker and Maddox[10] computed the distribution of local densities around an attractive Lennard-Jones solute ($\epsilon_{12}/\epsilon_{11} = 6.0$; $\sigma_{12}/\sigma_{11} = 1$) in the two-dimensional Lennard-Jones solvent, again at $T_r \approx 1.17$ and $\rho_r \approx 0.86$, and found the distribution to be about 20% narrower than around a solvent atom under the same conditions. Also, the maximum local density around the solute was shifted to higher densities, from ~0.4 Lennard-Jones units for the pure solvent, to ~0.5, consistent with the increased average local density expected around attractive solutes. A similar methodology was employed earlier by Randolph, O'Brien, and co-workers[62] to examine the fluctuations in an attractive three-dimensional Lennard-Jones solute−solvent system at $T_r = 1.08$ ($\epsilon_{12}/\epsilon_{11} = 1.5$; $\sigma_{12}/\sigma_{11} = 1.32$). These authors considered the standard deviation over 20 simulation runs of the *average* local density (using a cutoff $R = 3.0\sigma$) around the solute computed from "short" runs of 67 ps (10 000 time steps). They found that the fluctuations were large and that they were maximal at a bulk density of $\rho_r \approx 0.6$. In conflict with the results of Tucker and Maddox,[10] these authors found the density fluctuations around a tagged solvent atom to be much smaller than around the solute. However, the standard deviation method used by these authors is sensitive to the environment fluctuation time scales, i.e. if local environments interconvert frequently on the 67 ps time scale, their fluctuations will be averaged out, a complication which is not present in the local environment distribution function method of Tucker and Maddox, and it is possible that this is the source of the discrepancy between the two studies.

Another perspective from which the distribution of environments in compressible SCFs can be viewed is the consideration of the distribution of cluster sizes present in the fluid. Such distributions have been examined on the basis of both geometrically[176] and energetically[66,113] defined clusters, and this methodology has been applied to clusters involving attractive, repulsive and neutral (tagged solvent) solutes. It is observed that repulsive solutes are found in small clusters (e.g. 95% are found in clusters having one or fewer solvent atoms in a three-dimensional Lennard-Jones SCF at $T_r = 1.04$, $\rho_r = 1.0$),[113] neutrals are found in moderate clusters, and attractive solutes in large clusters (e.g. 90% are found in clusters with over 20 solvent atoms, and of these nearly 10% are

in clusters of larger than 150 solvent atoms).[113] However, such distributions do not provide immediate information about the *local* environments surrounding solutes.

2. Experiment

Nonexponential decay of dynamic solute processes, translating into a distribution of relaxation lifetimes, generally signals the presence of an inhomogeneous distribution of solvent environments around the solute. We note that although simulations have predicted that a distribution of lifetimes should be apparent in solute vibrational relaxation under some SC conditions,[68] this has not yet been observed.[94,100,101] However, Clouter et al.[184] have suggested that a distribution of dephasing lifetimes is responsible for line broadening observed in the vibrational Raman spectra of near-critical SC N_2. Additionally, such lifetime distributions have been observed in three studies of fluorescence emission from probe solutes in SCF solvents.[78,178,179] Rhodes and Fox[178] used single photon counting measurements to examine time-resolved fluorescence decay traces from phenanthracene in SC CO_2 at $T_r = 1.003$ and 1.01 for $0.6 < \rho_r < 2$. In all cases (of low solute concentration), multiexponentials were required to fit the decay traces, and three lifetime groups were observed. (It is worth noting that the authors performed a thorough analysis of their fitting procedure and found their main conclusions—the mean values and existence of three main lifetimes—to be robust, remaining the same whether 3 or 200 exponentials were used in the fits.) At the more near critical temperature of $T_r = 1.003$, the three lifetimes groupings appear to be of approximately equal importance. At $T_r = 1.01$, however, the longest lifetime group dominates the lifetime distribution, although the distribution of this group itself remains broad, with a full-width at half-maximum spanning tens of nanoseconds. Additionally, the pressure dependence at the lower temperature is much stronger than at the higher temperature. Specifically, at $T_r = 1.003$ the value of the lifetime which makes the maximal contribution to its group is <1 ns, ~6 ns, and ~35 ns for the three groups at $\rho_r = 1.14$. These decrease to <1 ns, ~5 ns, and ~23 ns at $\rho_r = 1.90$. Additionally, the lifetime groupings become somewhat less distinct at the highest density. In contrast, at $T_r = 1.01$, the maximal contribution to the dominant group shifts only from ~45 ns to ~41 ns as the density is increased from $\rho_r = 0.63$ to $\rho_r = 1.86$. While the data was interpreted as reflecting a distribution of local environments, there is at present no detailed understanding of these results. Note that solute−solute effects have not been ruled out and may be implicated even in these lower solute concentration studies.

Bright and co-workers[78,179] used both time-resolved fluorescence emission and multifrequency phase-modulation fluorescence spectroscopy to observe fluorescence emission lifetimes of PRODAN[78] in CHF_3 at $\rho_r = 1.25$ and $1.013 \leq T_r \leq 1.10$. From both sets of experiments, a Lorentzian distribution of lifetimes was found to best reproduce the data at each state point (although the residual for the Lorentzian fit, $\chi^2 = 1.03$, was only slightly better than that for a biexponential fit, $\chi^2 = 1.13$, at $T_r = 1.013$).[78] Additionally, the fits from the two experiments were found to agree well with one another. As a function of increasing temperature, the central lifetime was found to decrease from 3.9 ns at $T_r = 1.013$ to 1.9 ns at $T_r = 1.10$, while the full-width at half-maximum decreased only slightly, from 3.2 to 2.8 ns. Again, the lifetime distributions were attributed to the presence of an inhomogeneous distribution of local environments. Note that the presence of *average* local density enhancements, which are expected to be present when the distribution is broad (see above), were also confirmed in this system.[179]

C. Local Environment Lifetimes

An important quantity for assessing the influence that fluctuations in the local environments, i.e. fluctuations in the local densities, will have on dynamic solute processes is the time scale on which the local environments interconvert. A few molecular dynamics simulation studies have addressed this questions,[10,62,66,68,80,113,167,176] but the systems and state points which have been considered are few, and the specific solute processes considered differ. In particular, lifetimes for persistence of the number of solvent molecules (independent of identity) within some local region around the solute have been considered,[10,62] as have been lifetimes for persistence of the identity of the solvent molecules within such a local region.[80,113,167,180] Additionally, more global perspectives have been considered, in which the time scales for the loss of particle identity in extended cluster structures have been examined.[66,113,176]

Tucker and Maddox[10] examined a local density autocorrelation function in which the correlated variable is the instantaneous deviation of the local density around a specified particle away from the ensemble average of this local density. Here, the local density was defined as the number density of the solvent atoms within $R = 3.1\sigma$ of the specified particle. In pure two-dimensional, Lennard-Jones Ar at a high temperature where density inhomogeneities are not present, $T_r \approx 10.6$, the local density correlation function was found to decay rapidly, relaxing to half its initial value within 1 ps. At a near-critical temperature where density inhomogeneities are large in this two-dimensional system, $T_r \approx 1.17$, it takes ~19 ps for the local density correlation function to decay to half of its initial value. Recent work examining this relaxation time for various bulk densities along the $T_r \approx 1.17$ isotherm[64,68] show that the decay time decreases dramatically as one moves to high densities, indicating that the long local density lifetime at $\rho_r \approx 0.86$ is a direct consequence of the critical fluctuations, and not simply a reflection of the decreased temperature. Tucker and Maddox[10] also observed the local density fluctuations around an attractive Lennard-Jones solute in this system ($T_r \approx 1.17$, $\rho_r \approx 0.86$) and found them to decay more rapidly than do those around a tagged solvent particle, especially during the initial fast relaxation.

Inomata, Saito, and Debenedetti[167] also considered the decay of the local solvent environment, but these authors considered the time scale over which the identity of the particles within the local region, here

defined according to the first minimum in the radial distribution function, is lost. For molecular models of benzene in SC CO_2 at $T_r = 1.05$, the lifetimes extracted from the long time exponential decay of the identity persistence functions were found to increase with increasing bulk density ($0.5 \leq \rho_r \leq 2$), and to show no anomalous behavior near the critical density. Additionally, raising the temperature to $T_r = 1.10$ had negligible effect. Hence, it seems that unlike the lifetimes considered by Tucker and Maddox,[10] these identity lifetimes are not strongly affected by critical inhomogeneities (or that such inhomogeneities are small under the conditions considered). Likely candidates for this difference in behavior are the different natures of the lifetimes considered, i.e. solvent identity vs solvent density, the different ranges used to define "local" in the two studies, or the fact that one of the systems studied is more attractive than the other. Rossky, Johnston, and co-workers[80] also examined first-shell identity-persistence lifetimes.[180] These authors observed identity-persistence lifetimes on the order of a few picoseconds for solvent molecules around the chloride ion in three reaction complexes along the $Cl^- + CH_3Cl$ reaction path in SC water at $T_r = 1.0$ and $\rho_r = 1.5$. They found that the lifetimes were nearly a factor of 2 longer in those complexes having a negatively charged Cl^- than they were in the complex having a more dispersed charge distribution, a result attributed to the stronger Cl^-–H_2O interactions in the former complexes.

Debenedetti and co-workers[66,113] examined identity-persistence lifetimes for large, energetically defined clusters, i.e. contiguous networks of energetically bound atom pairs which include the solute (or tagged solvent), containing at least 60 solvent atoms, for both an attractive (Xe in Ne) and a pure (Ne in Ne) solute–solvent Lennard-Jones fluid at $T_r = 1.08$ and $\rho_r = 1.0$. Note that the observed lifetimes were found to be uncorrelated with the initial cluster size. The mean identity decay time around the attractive solute was found to be greater than 1.9 ps (this result was limited by the simulation run times of 2.1 ps per initial cluster), whereas around a tagged solvent atom it was found to be 0.54 ps, 3.5 times shorter. This is again in contrast to the local density correlation times computed by Tucker and Maddox,[10] which were observed to be, if anything, shorter around an attractive solute. However, both the systems and the nature of the lifetimes considered were different in these studies, so the results are intriguing, but not necessarily conflicting. Debenedetti and co-workers[113] also looked at the identity persistence time of solvent atoms local to the tagged particle, but only for single trajectories, so no lifetimes could be extracted.

A more global view of environmental relaxation was also taken by Yosii and Okazaki,[176] who examined contiguous networks of geometrically bound solvent pairs in a pure three-dimensional Lennard-Jones SCF at $T_r \approx 1.03$. These authors considered a bond-identity correlation function which follows the number of bonds remaining between atoms that originally constituted one cluster at time $t = 0$. After a rapid initial decay of ~1 ps attributed to "bond flickering," a longer time exponential decay was observed. It was found that the associated lifetime increased logarithmically with cluster size, and, since the cluster networks grow larger near the critical density, the slowest relaxations were observed at the near critical densities. It will be interesting in the future to relate these different viewpoints, both global and local, of the solvent dynamics in compressible SCFs, as well as to evaluate the usefulness of the many possible relaxation identifiers, such as local density and geometric identity.

V. Conclusions

There is no question that local density inhomogeneities and, in particular, local density enhancements, are a real and important phenomena in compressible SCFs, as evidenced by the numerous spectroscopic and computational determinations of these effects reviewed herein. However, while it appears that we have a qualitative understanding of the pressure and temperature dependence of local density enhancements and their effects on various measurable properties, this is where our present understanding ends. Numerous questions remain as to the factors which control the range of thermodynamic conditions over which density enhancements will be important. For example, what is the role of the detailed interaction potentials in determining this range? Or, for that matter, how do the potentials affect the spatial extent of these density fluctuations? What is the sensitivity, and the length scale of this sensitivity, of different experimental probes to local density enhancements? Additionally, we have just begun to investigate the detailed nature of these inhomogeneities. What are their spatial asymmetries? How do they fluctuate in time, and over what time scales? How does the microscopic, solute-centered view of the local density inhomogeneities fit into the more global picture of the solvent's near-critical density fluctuations? These are just some of the outstanding questions about solute density inhomogeneities in compressible SCFs, the answers to which will, perhaps, guide us in the use of solvent compressibility as an additional variable in the control of chemical processes.

VI. Acknowledgments

S.C.T. thanks Doug Henderson for helpful discussions and Grant Goodyear for creating the original figures and gratefully acknowledges an NSF Young Investigator Award and a Camille Dreyfus Teacher–Scholar Award. This work was supported by the National Science Foundation under Grant CHE-9727361.

VII. References

(1) McHugh, M. A.; Krukonis, V. J. *Supercritical Fluids Extraction: Principles and Practice*, 2nd ed.; Butterworths: Boston, 1994.
(2) Savage, P. E.; Gopalan, S.; Mizan, T. I.; Martino, C. J.; Brock, E. E. *AIChE J.* **1995**, *41*, 1723.
(3) Brennecke, J. F. *Chem. Ind.* **1996**, 831.
(4) Eckert, C. A.; Knutson, B. L.; Debenedetti, P. G. *Nature* **1996**, *383*, 313.
(5) Jessop, P. G.; Ikariya, T.; Noyori, R. *Science* **1995**, *269*, 1065.
(6) Wu, B. C.; Klein, M. T.; Sandler, S. I. *Ind. Eng. Chem. Res.* **1991**, *30*, 822.
(7) Antal, M. J., Jr.; Brittain, A.; DeAleida, C.; Ramayya, S.; Roy, J. C. In *Supercritical Fluids*; Squires, T. G. and Paulaitis, M.

E., Eds.; ACS Symposium Series 329, American Chemical Society: Washington, 1987.
(8) Johnston, K. P.; Haynes, C. *AIChE J.* **1987**, *33*, 2017.
(9) Stanley, H. E. *Phase Transitions and Critical Phenomena*; Clarendon Press: Oxford, 1987.
(10) Tucker, S. C.; Maddox, M. W. *J. Phys. Chem. B* **1998**, *102*, 2437.
(11) The scaling axis is the analytic continuation of the gas−liquid coexistence curve into the supercritical regime.
(12) Fisher, M. E. In *Critical Phenomena*; Proceeding, Stellenbosch, South Africa; Lecture Notes in Physics 186; Hahne, F. J. W., Ed.; Springer-Verlag: Stellenbosh, South Africa, 1983.
(13) Even in the absence of critical fluctuations one may see short length scale (generally first solvation shell) density inhomogeneities (typically enhancements) as a direct consequence of the intermolecular forces; such effects are frequently important at low densities. The relationship between local density enhancements which may arise in the absence of critical fluctuations and those which are a direct consequence of critical fluctuations is not very well understood. Observed density enhancements will most probably reflect both possible origins, with the relative importance of each being dependent upon the state point being considered and the strength of the attractive solute−solvent interactions. Some initial efforts aimed at understanding this relationship can be found in ref 64.
(14) Chialvo, A. A.; Debenedetti, P. G. *Ind. Eng. Chem. Res.* **1992**, *31*, 1391.
(15) Wu, R.-S.; Lee, L. L.; Cochran, H. D. *Ind. Eng. Chem. Res.* **1990**, *29*, 977.
(16) Debenedetti, P. G.; Chialvo, A. A. *J. Chem. Phys.* **1992**, *97*, 504.
(17) Zhang, J.; Lee, L. L.; Brennecke, J. F. *J. Phys. Chem.* **1995**, *99*, 9268.
(18) Roberts, C. B.; Zhang, J.; Chateauneuf, J. E.; Brennecke, J. F. *J. Am. Chem. Soc.* **1995**, *117*, 6553.
(19) Randolph, T. W.; O'Brien, J. A.; Ganapathy, S. *J. Phys. Chem.* **1994**, *98*, 4173.
(20) Ganapathy, S.; O'Brien, J. A.; Randolph, T. W. *AIChE J.* **1995**, *41*, 346.
(21) Ganapathy, S.; O'Brien, J. A.; Randolph, T. W. *J. Supercrit. Fluids* **1996**, *9*, 51.
(22) Yuan, H.; Gao, G. T.; Zeng, X. C. *Fluid Phase Equilib.* **1997**, *138*, 61.
(23) Roberts, C. B.; Brennecke, J. F.; Chateauneuf, J. E. *Thermodynamics* **1995**, *41*, 1306.
(24) Ellington, J. B.; Park, K. M.; Brennecke, J. F. *Ind. Eng. Chem. Res.* **1994**, *33*, 965.
(25) Kazarian, S. G.; Gupta, R. B.; Clarke, M. J.; Johnston, K. P.; Poliakoff, M. *J. Am. Chem. Soc.* **1993**, *115*, 11099.
(26) Randolph, T. W.; Blanch, H. W.; Prausnitz, J. M. *AIChE J.* **1988**, *34*, 1354.
(27) Schulte, R. D.; Kauffman, J. F. *Appl. Spectrosc.* **1995**, *49*, 31.
(28) Schulte, R. D.; Kauffman, J. F. *J. Phys. Chem.* **1994**, *98*, 8793.
(29) Kim, S.; Johnston, K. P. *AIChE J.* **1987**, *33*, 1603.
(30) Levelt-Sengers, J. M. H. In *Supercritical Fluid Technologies*; Bruno, T. J., Ely, J. F., Eds.; CRC Press: Boca Raton, 1991, p 1.
(31) Levelt-Sengers, J. M. H. *J. Supercrit. Fluids* **1991**, *4*, 215.
(32) Kajimoto, O. *Chem. Rev.* **1999**, *99*, 355 (this issue).
(33) O'Shea, K. E.; Kirmse, K. M.; Fox, M. A.; Johnston, K. P. *J. Phys. Chem.* **1991**, *95*, 7863.
(34) Bennett, G. E.; Johnston, K. *J. Phys. Chem.* **1994**, *98*, 441.
(35) Gupta, R. B.; Johnston, K. P. *Ind. Eng. Chem. Res.* **1994**, *33*, 2819.
(36) Cummings, P. T.; Chialvo, A. A.; Cochran, H. D. *Chem. Eng. Sci.* **1994**, *49*, 2735.
(37) Postorino, P.; Tromp, R. H.; Ricci, M. A.; Soper, A. K.; Neilson, G. W. *Nature* **1993**, *366*, 668.
(38) Mountain, R. *J. Chem. Phys.* **1989**, *90*, 1866.
(39) Mizan, T. I.; Savage, P. E.; Ziff, R. M. *J. Phys. Chem.* **1996**, *100*, 403.
(40) Chialvo, A. A.; Cummings, P. T. *J. Phys. Chem.* **1996**, *100*, 1309.
(41) Chialvo, A. A.; Cummings, P. T. *J. Chem. Phys.* **1994**, *101*, 4466.
(42) Johnston, K. P.; Kim, S.; Combes, J. In *Supercritical Fluid Science and Technology*; Johnston, K. P., Penninger, J. M. L., Eds.; ACS Symposium Series 406; American Chemical Society: Washington, 1989.
(43) Brennecke, J. F.; Eckert, C. A. *AIChE J.* **1989**, *35*, 1409.
(44) McNally, M. E. P.; Bright, F. V. In *Supercritical Fluid Technology*; McNally, M. E. P., Bright, F. V., Eds.; ACS Symposium Series 488; American Chemical Society: Washington, 1992.
(45) Carlier, C.; Randolph, T. W. *AIChE J.* **1993**, *39*, 876.
(46) Knutson, B. L.; Tomasko, D. L.; Eckert, C. A.; Debenedetti, P. G.; Chialvo, A. A. In *Supercritical Fluid Technology*; Bright, F. V., McNally, M. E., Eds.; ACS Symposium Series 488; American Chemical Society: Washington, 1992; p 60.
(47) Chialvo, A. A.; Cummings, P. T. *AIChE J.* **1994**, *40*, 1558.
(48) Herein I assume the case of infinitely dilute solution such that solute−solute correlations can be neglected. Specifically, as the solute density goes to zero, indirect interactions of the form solute i ($\mathbf{r}_1$) → solute j ($\mathbf{r}_2$) → solvent k ($\mathbf{r}_3$), which could alter the solvent density ar $\mathbf{r}_3$, can be neglected. This is analogous to neglecting terms of the form $\rho_u \int c_{u_1u_2}(\mathbf{r}_{12}) h_{u_2v_3}(\mathbf{r}_{23})\, d\mathbf{r}_2$ (u = solute and v = solvent) in the binary mixture Ornstein−Zernike equation[181] as $\rho_u \to 0$.
(49) Debenedetti, P. G. *Chem. Eng. Sci.* **1987**, *42*, 2203.
(50) Reference 10 errs in this regard.
(51) Hansen, J. P.; McDonald, I. R. *Theory of Simple Liquids*; Academic Press: London, 1986.
(52) Although measurements of partial molar properties contain contributions from both short- and long-range density inhomogeneities, the contribution of the long-range inhomogeneities diverges with the compressibility. As a result, the short-range contribution to partial molar properties becomes inconsequential as the critical point is approached.
(53) Krichevskii, I. R. *Russ. J. Phys. Chem.* **1967**, *41*, 1332.
(54) Rozen, A. M. *Russ. J. Phys. Chem.* **1976**, *50*, 1381.
(55) Khazanova, N. E.; Sominskaya, E. E. *Russ. J. Phys. Chem.* **1971**, *45*, 1485.
(56) Eckert, C. A.; Ziger, D. H.; Johnston, K. P.; Kim, S. *J. Phys. Chem.* **1986**, *90*, 2738.
(57) Biggerstaff, D. R.; Wood, R. H. *J. Phys. Chem.* **1988**, *92*, 1988.
(58) McGuigan, D. B.; Monson, P. A. *Fluid Phase Equilib.* **1990**, *57*, 227.
(59) Chimowitz, E. H.; Afrane, G. *Fluid Phase Equilib.* **1996**, *120*, 167.
(60) Sun, Y. P.; Fox, M. A.; Johnston, K. P. *J. Am. Chem. Soc.* **1992**, *114*, 1187.
(61) Tom, J. W.; Debenedetti, P. G. *Ind. Eng. Chem. Res.* **1993**, *32*, 2118.
(62) O'Brien, J. A.; Randolph, T. W.; Carlier, C.; Ganapathy, S. *AIChE J.* **1993**, *39*, 876.
(63) Brennecke, J. F.; Debenedetti, P. G.; Eckert, C. A.; Johnston, K. P. *AIChE J.* **1990**, *36*, 1927.
(64) Goodyear, G.; Maddox, M.; Tucker, S. C. Manuscript in preparation.
(65) Debenedetti, P. G.; Mohamed, R. S. *J. Chem. Phys.* **1989**, *90*, 4528.
(66) Debenedetti, P. G.; Petsche, I. B.; Mohamed, R. S. *Fluid Phase Equilib.* **1989**, *52*, 347.
(67) Petsche, I. B.; Debenedetti, P. G. *J. Phys. Chem.* **1991**, *95*, 386.
(68) Goodyear, G.; Tucker, S. C. *J. Chem. Phys.*, in press.
(69) Wu, R.-S.; Lee, L. L.; Cochran, H. D. *J. Supercrit. Fluids* **1992**, *5*, 192.
(70) The partial molar volume of a solute at infinite dilution can be written as the sum of two contributions. The first is the finite solvent−partial molar volume, i.e. the volume change that would result from addition of a solvent molecule. The second contribution arises because the solvent environment induced by the introduction of a solute molecule differs from the environment found around a solvent molecule. Note that as a result of indirect effects, the environment around solute and solvent molecules may differ out to very long distances from the central molecule. As a result, this second contribution scales as the isothermal compressibility of the solvent, and it diverges at the solvent's critical point.
(71) Zhang, J.; Roek, D. P.; Chateauneuf, J. E.; Brennecke, J. F. *J. Am. Chem. Soc.* **1997**, *119*, 9980.
(72) Sun, Y.-P.; Bunker, C. E.; Hamilton, N. B. *Chem. Phys. Lett.* **1993**, *210*, 111.
(73) Kajimoto, O.; Futakami, M.; Kobayashi, T.; Yamasaki, K. *J. Phys. Chem.* **1988**, *92*, 1347.
(74) Sun, Y.-P.; Bunker, C. E. *Ber. Bunsen-Ges. Phys. Chem.* **1995**, *99*, 976.
(75) Maroncelli, M. Personal communication.
(76) Flanagin, L. W.; Balbuena, P. B.; Johnston, K. P.; Rossky, P. J. *J. Phys. Chem. B* **1997**, *101*, 7998.
(77) Wallen, S. L.; Palmer, B. J.; Fulton, J. L. *J. Chem. Phys.* **1998**, *108*, 4039.
(78) Betts, T. A.; Zagrobelny, J.; Bright, F. V. *J. Supercrit. Fluids* **1992**, *5*, 48.
(79) Myers, D. J.; Urdahl, R. S.; Cherayil, B. J.; Fayer, M. D. *J. Chem. Phys.* **1997**, *107*, 9741.
(80) Flanagin, L. W.; Balbuena, P. B.; Johnston, K. P.; Rossky, P. J. *J. Phys. Chem.* **1995**, *99*, 5196.
(81) Cui, S. T.; Harris, J. G. *Chem. Eng. Sci.* **1994**, *49*, 2749.
(82) Rovere, M.; Heermann, D. W.; Binder, K. *J. Phys. Condens. Matter* **1990**, *2*, 7009.
(83) Smith, R. D.; Frye, S. L.; Yonker, C. R.; Gale, R. W. *J. Phys. Chem.* **1987**, *91*, 3059.
(84) Yonker, C. R.; Smith, R. D. *J. Phys. Chem.* **1988**, *92*, 235.
(85) McRae, E. G. *J. Phys. Chem.* **1957**, *61*, 526.
(86) Kim, S.; Johnston, K. P. *Ind. Eng. Chem. Res.* **1987**, *26*, 1206.
(87) Kim, S.; Johnston, K. P. In *Supercritical Fluids*; Squires, T. G., Paulaitis, M. E., Eds.; ACS Symposium Series 329; American Chemical Society: Washington, 1987.
(88) Ikushima, Y.; Saito, N.; Arai, M. *J. Phys. Chem.* **1992**, *96*, 2293.
(89) Ganapathy, S.; Carlier, C.; Randolph, T. W.; O'Brien, J. A. *Ind. Eng. Chem. Res.* **1996**, *35*, 19.
(90) Sun, Y.-P.; Fox, M. A. *J. Am. Chem. Soc.* **1993**, *115*, 3340.

(91) Morita, A.; Kajimoto, O. *J. Phys. Chem.* **1990**, *94*, 6420.
(92) Sun, Y.-P. *J. Phys. Chem.* **1993**, *97*, 282.
(93) Rice, J. K.; Niemeyer, E. D.; Dunbar, R. A.; Bright, F. V. *J. Am. Chem. Soc.* **1995**, *117*, 5830.
(94) Schwarzer, S.; Troe, J.; Zerezke, M. *J. Chem. Phys.* **1997**, *107*, 8380.
(95) Rice, J. K.; Niemeyer, E. D.; Bright, F. V. *J. Phys. Chem.* **1996**, *100*, 8499.
(96) Reynolds, L.; Gardecki, J. A.; Frankland, S. J. V.; Horng, M. L.; Maroncelli, M. *J. Phys. Chem.* **1996**, *100*, 10337.
(97) Sun, Y.-P.; Bennett, G.; Johnston, K. P.; Fox, M. A. *J. Phys. Chem.* **1992**, *96*, 10001.
(98) Betts, T. A.; Zagrobelny, J.; Bright, F. V. *J. Am. Chem. Soc.* **1992**, *114*, 8163.
(99) Heitz, M. P.; Maroncelli, M. *J. Phys. Chem. A* **1997**, *101*, 5852.
(100) Urdahl, R. S.; Myers, D. J.; Rector, K. D.; Davis, P. H.; Cherayil, B. J.; Fayer, M. D. *J. Chem. Phys.* **1997**, *107*, 3747.
(101) Urdahl, R. S.; Rector, K. D.; Myers, D. J.; Davis, P. H.; Fayer, M. D. *J. Chem. Phys.* **1996**, *105*, 8973.
(102) Cherayil, B. J.; Fayer, M. D. *J. Chem. Phys.* **1997**, *107*, 7642.
(103) Ikawa, S.; Fujita, Y. *J. Phys. Chem.* **1993**, *97*, 10607.
(104) Dong, D. C.; Winnik, M. A. *Can. J. Chem.* **1984**, *62*, 2560.
(105) Brennecke, J. F.; Tomasko, D. L.; Peshkin, J.; Eckert, C. A. *Ind. Eng. Chem. Res.* **1990**, *29*, 1682.
(106) Note that in ref 72 there is significant scatter in the data, while in ref 93 the supposedly same data presented in both Figures 13 and 14 of this reference is not self-consistent.
(107) Chen, S.-H.; McGuffin, V. L. *Appl. Spectrosc.* **1994**, *48*, 596.
(108) Wada, N.; Saito, M.; Kitada, D.; Smith, R. L., Jr.; Inomata, H.; Arai, K.; Saito, S. *J. Phys. Chem. B* **1997**, *101*, 10918.
(109) Chialvo, A. A.; Cummings, P. T. *Mol. Phys.* **1995**, *84*, 41.
(110) Chialvo, A. A.; Kalyuzhnyi, Y. V.; Cummings, P. T. *AIChE J.* **1996**, *42*, 571.
(111) Chialvo, A. A.; Cummings, P. T.; Simonson, J. M.; Mesmer, R. E. *J. Chem. Phys.* **1996**, *105*, 9248.
(112) Chialvo and Cummings'[47] expression for the free energy of solvation is written relative to the free energy of the ideal solution.
(113) Petsche, I. B.; Debenedetti, P. G. *J. Chem. Phys.* **1989**, *91*, 7075.
(114) Katagiri, M.; Tanaka, M.; Takaba, H.; Miyamoto, A.; Nozue, Y.; Terasaki, O.; Quirke, N.; Newsam, J. M. *Fluid Phase Equilib.* **1996**, *125*, 1.
(115) Tanaka, H.; Shen, J. W.; Nakanishi, K.; Zeng, X. C. *Chem. Phys. Lett.* **1995**, *239*, 168.
(116) Zeng, X. C.; Shen, J. W.; Nakanishi, H. T. K.; Yuan, H. *Fluid Phase Equilib.* **1986**, *116*, 296.
(117) Liew, C. C.; Inomata, H.; Saito, S. *Fluid Phase Equilib.* **1995**, *104*, 317.
(118) Cochran, H. D.; Cummings, P. T.; Karaborni, S. *Fluid Phase Equilib.* **1992**, *71*, 1.
(119) Cummings, P. T.; Cochran, H. D.; Simonson, J. M.; Mesmer, R. E.; Karaborni, S. *J. Chem. Phys.* **1991**, *94*, 5606.
(120) Figure 7 of ref 119 and Figure 4a of ref 118 disagree.
(121) Martinez, H. L.; Ravi, R.; Tucker, S. C. *J. Chem. Phys.* **1996**, *104*, 1067.
(122) In ref 36, the curves in Figure 15 appear to have been mislabeled, see Figure 16.
(123) Seminario, J. M.; Concha, M. C.; Murray, J. S.; Politzer, P. *Chem. Phys. Lett.* **1994**, *222*, 25.
(124) Re, M.; Laria, D. *J. Phys. Chem. B* **1997**, *101*, 10494.
(125) Gao, J. *J. Am. Chem. Soc.* **1993**, *115*, 6893.
(126) Munoz, F.; Chimowitz, E. H. *Fluid Phase Equilib.* **1992**, *71*, 237.
(127) Although refs 47 and 46 consider the same system, pyrene in CO_2, with the same potential functions, they do not obtain the same $\tilde{\rho}_l(\rho_r)$ curves, even given the same choice of cutoff values. In particular, the maximum values attained for $\tilde{\rho}_l$ are nearly the same in the two studies, but the positions of the maxima occur at much higher densities in ref 47. Possible sources of this discrepancy are (1) the use of integral equations with the Percus−Yevick closure in ref 47, whereas molecular dynamics simulation was used in ref 46 and/or (2) the use of different choices for the excluded volume of the solute when computing $\tilde{\rho}_l$.
(128) Wood, R. H.; Carter, R. W.; Quint, J. R.; Majer, V.; Thompson, P. T.; Boccio, J. O. *J. Chem. Thermodyn.* **1994**, *26*, 225.
(129) Luo, H.; Tucker, S. C. *Theor. Chem. Acc.* **1997**, *96*, 84.
(130) Adams, J. E. *J. Phys. Chem. B* **1998**, *102*, 7455.
(131) Cramer, C. J.; Truhlar, D. G. In *Reviews in Computational Chemistry*; Boyd, D. B., Lipkowitz, K. B., Eds.; VCH: New York, 1995.
(132) Davis, M. E.; McCammon, J. A. *Chem. Rev.* **1990**, *90*, 509.
(133) Honig, B.; Sharp, K.; Yang, A. *J. Phys. Chem.* **1993**, *97*, 1101.
(134) Tucker, S. C.; Gibbons, E. M. In *Structure and Reactivity in Aqueous Solution*; Truhlar, D. G., Cramer, C. J., Eds.; ACS Symposium Series; American Chemical Society: Washington, 1994; p 196.
(135) Wood, R. H.; Quint, J. R.; Grolier, J.-P. E. *J. Phys. Chem.* **1981**, *85*, 3944.
(136) Quint, J. R.; Wood, R. H. *J. Phys. Chem.* **1985**, *89*, 380.
(137) Luo, H.; Tucker, S. C. *J. Phys. Chem.* **1996**, *100*, 11165.
(138) Bennett, G. E.; Rossky, P. J.; Johnston, K. *J. Phys. Chem.* **1995**, *99*, 16136.
(139) Johnston, K. P.; Bennett, G. E.; Balbuena, P. B.; Rossky, P. J. *J. Am. Chem. Soc.* **1996**, *118*, 6746.
(140) Luo, H.; Tucker, S. C. *J. Am. Chem. Soc.* **1995**, *117*, 11359.
(141) Wood, R. H.; Quint, J. R. *J. Phys. Chem.* **1989**, *93*, 936.
(142) Born, M. *Z. Phys.* **1920**, *1*, 45.
(143) Klapper, I.; Hagstrom, R.; Fine, R.; Sharp, K.; Honig, B. *Proteins* **1986**, *1*, 47.
(144) Luo, H.; Tucker, S. C. *J. Phys. Chem. B* **1997**, *101*, 1063.
(145) Flarsheim, W. M.; Bard, A. J.; Johnston, K. P. *J. Phys. Chem.* **1989**, *93*, 4234.
(146) The agreement in ref 141 is not as good, presumably because the simulation temperature was not corrected for the critical point of the water model used.
(147) Pomelli, C. S.; Tomasi, J. *J. Phys. Chem. A* **1997**, *101*, 3561.
(148) Balbuena, P. B.; Johnston, K. P.; Rossky, P. J. *J. Phys. Chem.* **1995**, *99*, 1554; *J. Am. Chem. Soc.* **1994**, *116*, 2689.
(149) Klein, M. T.; Mentha, Y. G.; Torry, L. A. *Ind. Eng. Chem. Res.* **1992**, *31*, 182.
(150) Anderton, R. M.; Kauffman, J. F. *J. Phys. Chem.* **1995**, *99*, 13759.
(151) Heitz, M. P.; Bright, F. V. *J. Phys. Chem.* **1996**, *100*, 6889.
(152) Bai, S.; Taylor, C. M. V.; Liu, F.; Mayne, C. L.; Pugmire, R. J.; Grant, D. M. *J. Phys. Chem. B* **1997**, *101*, 2923.
(153) Chen, S.; Miranda, D. T.; Evilia, R. F. *J. Supercrit. Fluids* **1995**, *8*, 255.
(154) Howdle, S. M.; Bagratashvili, V. N. *Chem. Phys. Lett.* **1993**, *214*, 215.
(155) Oref, I.; Tardy, D. C. *Chem. Rev.* **1990**, *90*, 1407.
(156) Weston, R. E.; Flynne, G. W. *Annu. Rev. Phys. Chem.* **1992**, *43*, 559.
(157) Harris, C. B.; Smith, D. E.; Russell, D. J. *Chem. Rev.* **1990**, *90*, 481.
(158) Moore, P.; Tokmakoff, A.; Keyes, T.; Fayer, M. D. *J. Chem. Phys.* **1995**, *103*, 3235.
(159) Schwarzer, S.; Troe, J.; Votsmeier, M.; Zerezke, M. *J. Chem. Phys.* **1996**, *105*, 3121.
(160) Benzler, J.; Linkersdörfer, S.; Luther, K. *J. Chem. Phys.* **1997**, *106*, 4992.
(161) Lee, M.; Hotom, G. R.; Hochstrasser, R. M. *Chem. Phys. Lett.* **1985**, *118*, 359.
(162) Hegarty, J. N. M.; McGarvey, J. J.; Bell, S. E. J.; Al-Obaidi, A. H. R. *J. Phys. Chem.* **1996**, *100*, 15704.
(163) Egorov, S. A.; Stephens, M. D.; Skinner, J. L. *J. Chem. Phys.* **1997**, *107*, 10485.
(164) Lamb, D. M.; Adamy, S. T.; Woo, K. W.; Jonas, J. *J. Phys. Chem.* **1989**, *93*, 5002.
(165) Umezawa, S.; Nagashimi, A. *J. Supercrit. Fluids* **1992**, *5*, 242.
(166) Iwai, Y.; Higashi, H.; Uchida, H.; Arai, Y. *Fluid Phase Equilib.* **1997**, *127*, 251.
(167) Inomata, H.; Saito, S.; Debenedetti, P. *Fluid Phase Equilib.* **1996**, *116*, 282.
(168) Luo, H.; Ciccotti, G.; Mareschal, M.; Meyer, M.; Zappoli, B. *Phys. Rev. E* **1995**, *51*, 2013.
(169) Nishiumi, H.; Fujita, M.; Agou, K. *Fluid Phase Equilib.* **1996**, *117*, 356.
(170) Baglin, F. G. Personal communication.
(171) Ben-Amotz, D.; LaPlant, F.; Shea, D.; Gardecki, J.; List, D. In *Supercritical Fluid Technology*; Bright, F. V., McNally, M. E., Eds.; ACS Symposium Series 488; American Chemical Society: Washington, 1992.
(172) Okazaki, S.; Matsumoto, M.; Okada, I. *J. Chem. Phys.* **1995**, *103*, 8549.
(173) Yagi, Y.; Tsugane, H.; Inomata, H.; Saito, S. *J. Supercrit. Fluids* **1993**, *6*, 139.
(174) Iwai, Y.; Koga, Y.; Arai, Y. *Fluid Phase Equilib.* **1996**, *116*, 267.
(175) Iwai, Y.; Uchida, H.; Koga, Y.; Arai, Y.; Mori, Y. *Ind. Eng. Chem. Res.* **1996**, *35*, 3782.
(176) Yoshii, N.; Okazaki, S. *J. Chem. Phys.* **1997**, *107*, 2020.
(177) The potentials used differ slightly, see refs 121 and 168.
(178) Rhodes, T. A.; Fox, M. A. *J. Phys. Chem.* **1996**, *100*, 17931.
(179) Betts, T. A.; Zagrobelny, J.; Bright, F. V. In *Supercritical Fluid Technology*; Bright, F. V., McNally, M. E. P., Eds.; ACS Symposium Series 488; American Chemical Society: Wasington, 1992.
(180) Note that Flanagin et al.'s[80] definition of the identity persistence time differs from that of refs 167 and 113.
(181) Friedman, H. L. *A Course in Statistical Mechanics*; Prentice Hall: Englewood Cliffs, NJ, 1985.
(182) deGrazia, J. L.; Randolph, T. W.; O'Brien, J. A. *J. Phys. Chem. A* **1998**, *102*, 1674.
(183) Kajimoto, O.; Sekiguchi, K.; Nayuki, T.; Kobayashi, T. *Ber. Bunsen-Ges. Phys. Chem.* **1997**, *101*, 600.
(184) Clouter, M. J.; Kiefte, H.; Deacon, C. G. *Phys. Rev. A* **1986**, *33*, 2749.

CR9700437